

## Response to Anonymous Referee #1

We appreciate your valuable comments and suggestion, which significantly improved the manuscript. We carefully answered them point-by-point as below and improved the corresponding parts in the manuscript.

Reviewer's comments are in plain face.

Author's responses are in blue color.

Changes in the manuscript are in red color.

The paper presents the first long-term datasets from the “Campaign on atmospheric Aerosol REsearch” network of China (CARE-China), including three years of observations of online PM<sub>2.5</sub> mass concentrations (2012-2014) and one year of observations of PM<sub>2.5</sub> compositions (2012-2013). The average PM<sub>2.5</sub> concentrations at 20 urban sites was three times higher than the average value from the 12 background sites. The PM<sub>2.5</sub> concentrations are generally higher in east-central China than in the other parts of the country due to their relative large particulate matter (PM) emissions and the unfavourable meteorological conditions for pollution dispersion. The seasonal variability of the PM<sub>2.5</sub> shows high values in winter and low values during summer at urban sites. Bimodal and unimodal diurnal variation patterns were identified at both urban and background sites. The chemical compositions of PM<sub>2.5</sub> at all urban sites are organic matter (OM), SO<sub>4</sub><sup>2-</sup>, mineral dust, NO<sub>3</sub><sup>-</sup>, NH<sub>4</sub><sup>+</sup>, elemental carbon (EC), Cl<sup>-</sup> at 45% RH and residual matter (20.7%). Similar chemical compositions of PM<sub>2.5</sub> were observed at background sites but were associated with higher fractions of OM and lower fractions of NO<sub>3</sub><sup>-</sup> and EC. Significant variations of the chemical species were observed among the sites. The PM<sub>2.5</sub> chemical species at the background sites exhibited larger spatial heterogeneities than those at urban sites. Six pairs of urban and background sites from each region of China were selected, and the differences in the chemical compositions of urban and background sites were analysed. It is suggested that there are different contributions from regional anthropogenic or natural emissions and from the long-range transport to background areas. Notable seasonal variations of PM<sub>2.5</sub> polluted days were observed, especially for the megacities in east-central China, resulting in frequent heavy pollution episodes occurring during winter.

[Response] Thank you very much for your comments.

### General comments

It is concluded from the similar evolution of the PM<sub>2.5</sub> chemical compositions on polluted days at the urban and nearby background sites that there are significant regional pollution characteristics of the most polluted areas of China. Following this it is stated that the chemical species dominating the evolutions of the heavily polluted events were different in these areas, indicating that unique mitigation measures should be developed for different regions of China. This is not conclusive and must be explained in more detail: What means “significant regional pollution characteristics of the most polluted areas of China” together with “chemical species dominating the

evolutions of the heavily polluted events were different in these areas”? What means “unique mitigation measures should be developed for different regions of China”? This more precise description is required due to the conclusion that the analyses provides insights into the sources, processes, and lifetimes of heavily polluted events.

The paper addresses relevant scientific tasks. The paper presents novel concepts, ideas and tools. The scientific methods and assumptions are valid and clearly outlined so that substantial conclusions are reached. The description of experiments and calculations allow their reproduction by fellow scientists. The quality of the figures is good. The figure captions should be improved so that these are understandable without the overall manuscript.

The related work is well cited so that the authors give proper credit to related work and own new contribution. The title as well as the abstract reflects the whole content of the paper. The overall presentation is well structured and clear. The language is fluent. The mathematical formulae, symbols, abbreviations, and units are generally correctly defined and used.

[Response] Thank you very much for your comments, and thanks for the affirmation of reviewer to our work.

(1) The “significant regional pollution characteristics of the most polluted areas of China” means fine particle pollution in the most polluted areas of China assumes a regional tendency, according to the consistent evolution of fine particle chemical composition between urban site and its nearby background site. Sorry for the misunderstanding. In addition, we admitted that “chemical species dominating the evolutions of the heavily polluted events were different in these areas” is ambiguous. To make it clear, we revised these sentences in the Abstract as showed below:

“The evolution of the PM<sub>2.5</sub> chemical compositions on polluted days was consistent for the urban and nearby background sites, where the sum of sulfate, nitrate and ammonia typically constituted much higher fractions (31-57%) of PM<sub>2.5</sub> mass, suggesting fine particle pollution in the most polluted areas of China assumes a regional tendency, and the importance to address the emission reduction of secondary aerosol precursors including SO<sub>2</sub> and NO<sub>x</sub>.”

(2) Sorry for the misunderstanding. We admitted that “unique mitigation measures should be developed for different regions of China” is ambiguous. To make it clear, more discussion about the major primary sources contributed to the high fine particle loading in specific regions was conducted in section 3.3.2. Based on these analysis, we revised the sentences as follow:

“Furthermore, distinct differences in the evolution of [NO<sub>3</sub><sup>-</sup>]/[SO<sub>4</sub><sup>2-</sup>] ratio and OC/EC ratio in polluted days imply that mobile sources and stationary (coal combustion) sources are likely more important in Guangzhou and Shenyang, respectively, whereas in Beijing it is mobile sources and biomass burning. As for Chongqing, the higher oxidation capacity than the other three cities suggested it should pay more attention to the emission reduction of secondary aerosol precursors.”

(3) The figure captions have been improved.

### Specific Comments:

Different instruments for measurements of PM<sub>2.5</sub> mass concentrations are applied at the different sites and well described. But what shows an intercomparison of these different types of instruments?

[Response] Thank you for your comments. In fact, the intercomparison of the different types of instruments had been done before the routine work of CARE-China network. First, we provide more details on the comparison of PM<sub>2.5</sub> mass concentration measured from two kinds of on-line instruments (TEOM and EBAM) used in this study, the results showed that these two on-line instruments correlated well ( $R^2=0.90$ ,  $P<0.001$ ). TEOM reported approximately 24% lower mass concentration than EBAM, and the difference could be explained by the loss of semi-volatile materials from TEOM (Zhu et al., 2007).

Second, the comparison of PM<sub>2.5</sub> mass concentration measured from filter sampling and the on-line instruments (TEOM and EBAM) during the one-year observation period was provided. On average, PM<sub>2.5</sub> mass concentrations measured by the filter sampling was approximately 9% higher than the on-line instruments. The discussions about the intercomparison was added in section 2.2 and the results was provided in the support information.

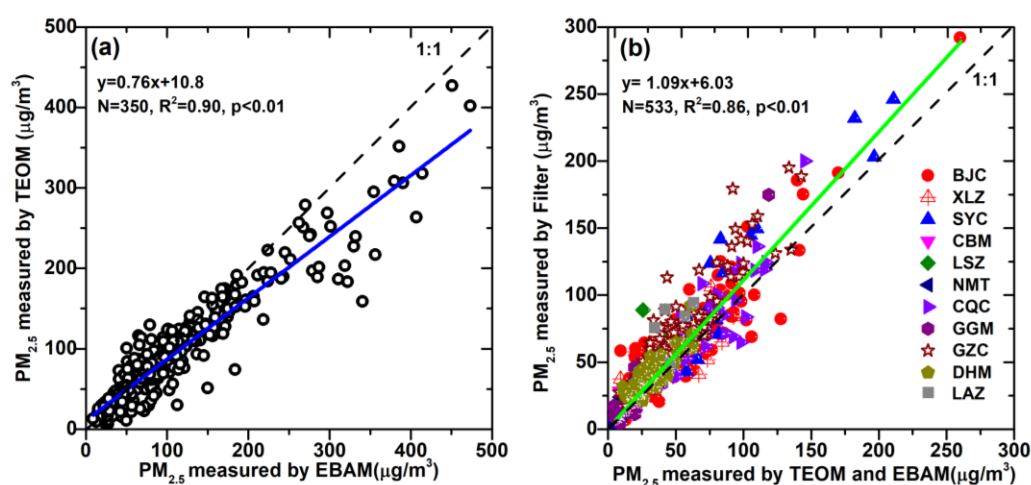


Fig. S1 (a) Intercomparison of PM<sub>2.5</sub> mass concentrations measured by the tapered element oscillating microbalance (TEOM) and the beta gauge instruments (EBAM) conducted at the Beijing site; (b) Intercomparison of PM<sub>2.5</sub> mass concentrations measured by filter sampling and the on-line instruments (TOEM and EBAM) from the 11 sites during the one-year observation period. (BJC: Beijing; XLZ: Xinglong; SYC: Shenyang; CBM: Changbai Mountain; LSZ: Lhasa; NMT: Namtso; CQZ: Chongqing; GGM: Gongga Mountain; GZC: Guangzhou; DHM: Dinghu Mountain; LAZ: Lin'an)

Zhu, K., Zhang, J., Lioy, P. J.: Evaluation and Comparison of Continuous Fine Particulate Matter Monitors for Measurement of Ambient Aerosols, *J. Air & Waste Manage. Assoc.*, 57:12, 1499-1506, 2007.

Chapter 4 is a summary with some conclusions. More detailed conclusions are possible and should be drawn.

[Response] Thank you for your comments. We revised Chapter 4, and more detailed conclusions from the chemical evolution of PM<sub>2.5</sub> composition in polluted days and the implication for the mitigation measures were drawn in the revised MS.

“...The increasing contribution of secondary aerosol on polluted days was observed both for the urban and nearby background sites, suggesting fine particle pollution in the most polluted areas of China assumes a regional tendency, and the importance to address the emission reduction of secondary aerosol precursors. In addition, the chemical species dominating the evolutions of the heavily polluted events were different, while decreasing or constantly contribution of OM associated with increasing contribution of SIA characteristic evolution of PM<sub>2.5</sub> in NCP, PRD and SWCR, the opposite phenomenon was observed in NECR. Further analysis from the [NO<sub>3</sub><sup>-</sup>]/[SO<sub>4</sub><sup>2-</sup>] ratio and OC/EC ratio showed that fine particle pollution in Guangzhou and Shenyang was mainly attributed to the traffic emissions and coal combustion, respectively, while more complex and variable major sources including mobile vehicle emission and residential sources contributed to the development of heavily polluted days in Beijing. As for Chongqing, the higher oxidation capacity than other cities suggested it should pay more attention to the emission reduction of secondary aerosol precursors. These results suggest the different formation mechanisms of the heavy pollution in the most polluted city clusters, and unique mitigation measures should be developed for the different regions of China.”

**Technical corrections:**

Unaccounted and residual matter is for the same in chemical composition. This should be explained – what does it mean? Some free spaces are missing in the figure captions.

[Response] Thank you for your comments. Yes, the unaccounted and residual matter are the same which both refer to the difference between the PM<sub>2.5</sub> gravimetric mass and the sum of the PM constituents (OM, EC, SO<sub>4</sub><sup>2-</sup>, NO<sub>3</sub><sup>-</sup>, NH<sub>4</sub><sup>+</sup>, Mineral dust and Cl<sup>-</sup>). The remaining unaccounted-for mass fraction may be the result of analytical errors, a systematic underestimation of the PM constituents whose concentrations are calculated from the measured data (e.g., OM, and mineral dust), and aerosol-bound water (especially when mass concentrations are determined at RH >30%). To make it clear, “residual matter” was replaced by “unaccounted” throughout the MS, for consistency. In addition, the figure captions have been improved.



1 **Characteristics of PM<sub>2.5</sub> mass concentrations and chemical species in urban and background**  
2 **areas of China: emerging results from the CARE-China network**

3 Zirui Liu<sup>1\*</sup>, Wenkang Gao<sup>1</sup>, Yangchun Yu<sup>1</sup>, Bo Hu<sup>1</sup>, Jinyuan Xin<sup>1</sup>, Yang Sun<sup>1</sup>, Lili Wang<sup>1</sup>, Gehui  
4 Wang<sup>3</sup>, Xinhui Bi<sup>4</sup>, Guohua Zhang<sup>4</sup>, Honghui Xu<sup>5</sup>, Zhiyuan Cong<sup>6</sup>, Jun He<sup>7</sup>, Jingsha Xu<sup>7</sup>, Yuesi  
5 Wang<sup>1,2\*</sup>

6 <sup>1</sup>State Key Laboratory of Atmospheric Boundary Layer Physics and Atmospheric Chemistry, Institute of  
7 Atmospheric Physics, Chinese Academy of Sciences, Beijing 100029, China

8 <sup>2</sup>Center for Excellence in Regional Atmospheric Environment, Institute of Urban Environment, Chinese Academy of  
9 Sciences, Xiamen 361021, China

10 <sup>3</sup>State Key Laboratory of Loess and Quaternary Geology, Institute of Earth Environment, Chinese Academy of  
11 Sciences, Xi'an 710075, China

12 <sup>4</sup>State Key Laboratory of Organic Geochemistry, Guangzhou Institute of Geochemistry, Chinese Academy of  
13 Sciences, Guangzhou 510640, China

14 <sup>5</sup>Zhejiang Meteorology Science Institute, Hangzhou 310017, China

15 <sup>6</sup>Key Laboratory of Tibetan Environment Changes and Land Surface Processes, Institute of Tibetan Plateau  
16 Research, Chinese Academy of Sciences, Beijing 100101, China

17 <sup>7</sup>International Doctoral Innovation Centre, The University of Nottingham Ningbo China, Ningbo 315100, China

18 \*Corresponding author: Z.R Liu (Liuzirui@mail.iap.ac.cn); Y.S Wang (wys@mail.iap.ac.cn)

19  
20 **Abstract:** The “Campaign on atmospheric Aerosol REsearch” network of China (CARE-China) is  
21 a long-term project for the study of the spatiotemporal distributions of physical aerosol  
22 characteristics as well as the chemical components and optical properties of aerosols over China.  
23 This study presents the first long-term datasets from this project, including three years of  
24 observations of online PM<sub>2.5</sub> mass concentrations (2012-2014) and one year of observations of  
25 PM<sub>2.5</sub> compositions (2012-2013) from the CARE-China network. The average PM<sub>2.5</sub>  
26 concentrations at 20 urban sites is 73.2 μg/m<sup>3</sup> (16.8-126.9 μg/m<sup>3</sup>), which was three times higher  
27 than the average value from the 12 background sites (11.2-46.5 μg/m<sup>3</sup>). The PM<sub>2.5</sub> concentrations  
28 are generally higher in east-central China than in the other parts of the country due to their relative  
29 large particulate matter (PM) emissions and the unfavorable meteorological conditions for  
30 pollution dispersion. A distinct seasonal variability of the PM<sub>2.5</sub> is observed, with highs in the  
31 winter and lows during the summer at urban sites. Inconsistent seasonal trends were observed at  
32 the background sites. Bimodal and unimodal diurnal variation patterns were identified at both  
33 urban and background sites. The chemical compositions of PM<sub>2.5</sub> at six paired urban and  
34 background sites located within the most polluted urban agglomerations (**North China Plain (NCP),**  
35 **Yangtze River Delta (YRD), Pearl River Delta (PRD), Northeast China Region (NECR),**  
36 **Southwestern China Region (SWCR))** and cleanest regions (**Tibetan Autonomous Region (TAR))**  
37 of China were analyzed. The major PM<sub>2.5</sub> constituents across all the urban sites are organic matter  
38 (OM, 26.0%), SO<sub>4</sub><sup>2-</sup>(17.7%), mineral dust (11.8%), NO<sub>3</sub><sup>-</sup> (9.8%), NH<sub>4</sub><sup>+</sup> (6.6%), elemental carbon  
39 (EC) (6.0%), Cl<sup>-</sup> (1.2%) at 45% RH and **unaccounted matter** (20.7%). Similar chemical  
40 compositions of PM<sub>2.5</sub> were observed at background sites but were associated with higher  
41 fractions of OM (33.2%) and lower fractions of NO<sub>3</sub><sup>-</sup> (8.6%) and EC (4.1%). Significant variations  
42 of the chemical species were observed among the sites. At the urban sites, the OM ranged from

43 12.6  $\mu\text{g}/\text{m}^3$  (Lhasa) to 23.3  $\mu\text{g}/\text{m}^3$  (Shenyang), the  $\text{SO}_4^{2-}$  ranged from 0.8  $\mu\text{g}/\text{m}^3$  (Lhasa) to 19.7  
44  $\mu\text{g}/\text{m}^3$  (Chongqing), the  $\text{NO}_3^-$  ranged from 0.5  $\mu\text{g}/\text{m}^3$  (Lhasa) to 11.9  $\mu\text{g}/\text{m}^3$  (Shanghai) and the EC  
45 ranged from 1.4  $\mu\text{g}/\text{m}^3$  (Lhasa) to 7.1  $\mu\text{g}/\text{m}^3$  (Guangzhou). The  $\text{PM}_{2.5}$  chemical species at the  
46 background sites exhibited larger spatial heterogeneities than those at urban sites, suggesting the  
47 different contributions from regional anthropogenic or natural emissions and from the long-range  
48 transport to background areas. Notable seasonal variations of  $\text{PM}_{2.5}$  polluted days were observed,  
49 especially for the megacities in east-central China, resulting in frequent heavy pollution episodes  
50 occurring during the winter. **The evolution of the  $\text{PM}_{2.5}$  chemical compositions on polluted days**  
51 **was consistent for the urban and nearby background sites, where the sum of sulfate, nitrate and**  
52 **ammonia typically constituted much higher fractions (31-57%) of  $\text{PM}_{2.5}$  mass, suggesting fine**  
53 **particle pollution in the most polluted areas of China assumes a regional tendency, and the**  
54 **importance to address the emission reduction of secondary aerosol precursors including  $\text{SO}_2$  and**  
55  **$\text{NO}_x$ . Furthermore, distinct differences in the evolution of  $[\text{NO}_3^-]/[\text{SO}_4^{2-}]$  ratio and OC/EC ratio in**  
56 **polluted days imply that mobile sources and stationary (coal combustion) sources are likely more**  
57 **important in Guangzhou and Shenyang, respectively, whereas in Beijing it is mobile emission and**  
58 **residential sources. As for Chongqing, the higher oxidation capacity than the other three cities**  
59 **suggested it should pay more attention to the emission reduction of secondary aerosol precursors.**  
60 This analysis reveals the spatial and seasonal variabilities of the urban and background aerosol  
61 concentrations on a national scale and provides insights into their sources, processes, and  
62 lifetimes.

63

## 64 **1. Introduction**

65 Atmospheric fine particulate matter ( $\text{PM}_{2.5}$ ) is a complex heterogeneous mixture, whose  
66 physical size distribution and chemical composition change in time and space and are dependent  
67 on the emission sources, atmospheric chemistry, and meteorological conditions (Seinfeld and  
68 Pandis, 2016). Atmospheric  $\text{PM}_{2.5}$  has known important environmental impacts related to visibility  
69 degradation and climate change. Because of their abilities to scatter and absorb solar radiation,  
70 aerosols degrade visibility in both remote and urban locations and can have direct and indirect  
71 effects on the climate (IPCC, 2013). Fine atmospheric particles are also a health concern and have  
72 been linked to respiratory and cardiovascular diseases (Sun et al., 2010; Viana et al., 2008; Zhang  
73 et al., 2014a). The magnitudes of the effects of  $\text{PM}_{2.5}$  on all these systems depend on their sizes  
74 and chemical compositions. Highly reflective aerosols, such as sulfates and nitrates, result in  
75 direct cooling effects, while aerosols with low single-scattering albedos absorb solar radiation and  
76 include light-absorbing carbon, humic-like substances, and some components of mineral soils  
77 (Hoffer et al., 2006). The health impacts of these particles may also differ with different aerosol  
78 compositions (Zimmermann, 2015); the adverse health effects specifically associated with organic  
79 aerosols have been reported by Mauderly and Chow (2008). Therefore, the uncertainties  
80 surrounding the roles of aerosols in climate, visibility, and health studies can be significant  
81 because chemical composition data may not be available for large spatial and temporal ranges.

82 Reducing the uncertainties associated with aerosol effects requires observations of aerosol  
83 mass concentrations and chemical speciation from long-term spatially extensive ground-based  
84 networks. Continental sampling using ground-based networks has been conducted in North

85 America (Hand et al., 2012) and Europe (Putaud et al., 2010) since the 1980s, such as via the U.S.  
86 EPA's Chemical Speciation Network (CSN), the Interagency Monitoring of Protected Visual  
87 Environments (IMPROVE) network, the Clean Air Status and Trends Network (CASTNET) and  
88 the National Atmospheric Deposition Program (NADP). Previous studies suggest the spatial and  
89 temporal patterns of PM<sub>2.5</sub> mass concentrations and chemical species can vary significantly  
90 depending on species and location. For example, Malm et al. (2004) reported the 2001 monthly  
91 mean speciated aerosol concentrations from the IMPROVE monitors across the United States and  
92 demonstrated that ammonium sulfate concentrations were highest in the eastern United States and  
93 dominated the fine particle masses in the summer. Clearly decreasing gradients of the SO<sub>4</sub><sup>2-</sup> and  
94 NO<sub>3</sub><sup>-</sup> contributions to PM<sub>10</sub> were observed in Europe when moving from rural to urban to kerbside  
95 sites (Putaud et al., 2010). Although large disparities of PM<sub>2.5</sub> pollution levels exist between those  
96 megacities in developing and developed countries, the PM<sub>2.5</sub> annual mass concentrations in the  
97 former are approximately 10 times greater than those of the latter (Cheng et al., 2016); however,  
98 ground-based networks that consistently measures PM<sub>2.5</sub> mass concentrations and chemical  
99 compositions remain rare in the densely populated regions of developing countries.

100 China is the world's most populous country and has one of the fastest-growing economies.  
101 Fast urbanization and industrialization can cause considerable increases in energy consumption.  
102 China's energy consumption increased 120% from 2000 to 2010. Coal accounted for most of the  
103 primary energy consumption (up to 70%) (Department of Energy Statistics, National Bureau of  
104 Statistics of China, 2001; 2011). Meanwhile, the emissions of high concentrations of numerous air  
105 pollutants cause severe air pollution and haze episodes. For example, a heavy air pollution episode  
106 occurred in northeastern China in January of 2013, wherein the maximum hourly averaged PM<sub>2.5</sub>  
107 exceeded 600 µg m<sup>-3</sup> in Beijing (Wang et al., 2014). This event led to considerable public concern.  
108 However, ground-based networks that consistently measure PM<sub>2.5</sub> mass concentrations and  
109 chemical compositions in China are limited. Although there were some investigations of the  
110 various aerosol chemical compositions in China (He et al., 2001; Huang et al., 2013; Li et al.,  
111 2012; Liu et al., 2015; Pan et al., 2013; Tao et al., 2014; Wang et al., 2013; Yang et al., 2011; Zhao  
112 et al., 2013a; Zhou et al., 2012), earlier studies were limited in their temporal and spatial scopes,  
113 with very few having data exceeding one year while covering various urban and remote regions of  
114 the country (Zhang et al., 2012; Wang et al., 2015b). Indeed, before 2013, the Chinese national  
115 monitoring network did not report measurements of PM<sub>2.5</sub> or its chemical composition, and thus,  
116 ground-based networks for atmospheric fine particulate matter measurements at regional and  
117 continental scales are needed as these networks are essential for the development and  
118 implementation of effective air pollution control strategies and are also useful for the evaluation of  
119 regional and global models and satellite retrievals.

120 To meet these sampling needs, the "Campaign on atmospheric Aerosol REsearch" network  
121 of China (CARE-China) was established in late 2011 for the study of the spatiotemporal  
122 distributions of the physical and chemical characteristics and optical properties of aerosols (Xin et  
123 al., 2015). This study presents the first long-term dataset to include three years of observations of  
124 online PM<sub>2.5</sub> mass concentrations (2012-2014) and one year of observations of PM<sub>2.5</sub> compositions  
125 (2012-2013) from the CARE-China network. The purpose of this work is to (1) assess the PM<sub>2.5</sub>  
126 mass concentration levels, including the seasonal and diurnal variation characteristics at the urban,

127 rural and regional background sites; to (2) obtain the seasonal variations of the PM<sub>2.5</sub> chemical  
128 compositions at paired urban/background sites in the most polluted regions and clean areas; and to  
129 (3) identify the occurrences and chemical signatures of haze events via an analysis of the temporal  
130 evolutions and chemical compositions of PM<sub>2.5</sub> on polluted days. These observations and analyses  
131 provide general pictures of atmospheric fine particulate matter in China and can also be used to  
132 validate model results and implement effective air pollution control strategies.

## 133 **2 Materials and methods**

### 134 **2.1 An introduction to the PM<sub>2.5</sub> monitoring sites**

135 The PM<sub>2.5</sub> data from 36 ground observation sites used in this study were obtained from the  
136 CARE-China network (Campaign on the atmospheric Aerosol REsearch network of China), which  
137 was supported by the Chinese Academy of Sciences (CAS) Strategic Priority Research Program  
138 grants (Category A). Xin et al. (2015) provided an overview of the CARE-China network, the  
139 cost-effective sampling methods employed and the post-sampling instrumental methods of  
140 analysis. Four more ground observation sites (Shijiazhuang, Tianjin, Ji'nan and Lin'an) from the  
141 "Forming Mechanism and Control Strategies of Haze in China" group (Wang et al., 2014) were  
142 also included in this study to better depict the spatial distributions and temporal variations of the  
143 PM<sub>2.5</sub> in eastern China. A comprehensive 3-year observational network campaign from 2012 to  
144 2014 was carried out at these 40 ground observation sites. Figure 1 and Table 1, respectively, show  
145 the geographic distribution and details of the network stations, which include 20 urban sites, 12  
146 background sites and 8 rural/suburban sites. The urban sites, such as those at Beijing, Shanghai  
147 and Guangzhou, are locations surrounded by typical residential areas and commercial districts.  
148 The background sites are located in natural reserve areas or scenic spots, which are far away from  
149 anthropogenic emissions and are less influenced by human activities. Rural/suburban sites are  
150 situated in rural and suburban areas, which may be affected by agricultural activities, vehicle  
151 emissions and some light industrial activities. These sites are located in different parts of China  
152 and can provide an integrated insight into the characteristic of PM<sub>2.5</sub> over China.

### 153 **2.2 Online instruments and data sets**

154 A tapered element oscillating microbalance (TEOM) was used for the PM<sub>2.5</sub> measurements at  
155 thirty-four sites within the network (Table S1). This system was designated by the US  
156 Environmental Protection Agency (USEPA) as having a monitoring compliance equivalent to the  
157 National Ambient Air Quality standard for particulate matter (Patashnick and Rupprecht 1991).  
158 The measurement ranges of the TEOMs were 0-5 g/m<sup>3</sup>, with a 0.1 µg/m<sup>3</sup> resolution and precisions  
159 of ±1.5 (1-h average) and ±0.5 µg/m<sup>3</sup>. The models used in the network are TEOM 1400a and  
160 TEOM 1405, and the entire system was heated to 50 °C; thus, a loss of semi-volatile compounds  
161 cannot be avoided. Our previous study showed that up to 25% lower mass concentrations were  
162 found for select daily means than those observed with gravimetric filter measurements, depending  
163 on the ammonium-nitrate levels and ambient temperatures (Liu et al., 2015). The errors of the  
164 TEOM measurements are systematic in that they are always negative. Thus, these errors may not  
165 be important for the study of the spatial distributions and temporal variations of PM<sub>2.5</sub>. The other  
166 six sites of the network (Shanghai, Guangzhou, Chengdu, Xi'an, Urumchi and Qinghai Lake) were  
167 equipped with beta gauge instruments (EBAM, Met One Instruments Inc., Oregon). The  
168 measurement range of EBAM is 0-1000 µg/m<sup>3</sup>, with a precision of 0.1 µg/m<sup>3</sup> and a resolution of

169 0.1  $\mu\text{g}/\text{m}^3$ . The filters were changed every week, and the inlet was cleaned every month. The flow  
170 rates were also monitored and concurrently calibrated. A year-long intercomparison of daily  $\text{PM}_{2.5}$   
171 mass concentrations measured by TEOM and EBAM was conducted at the Beijing site (Fig. S1a),  
172 and the results showed that these two on-line instruments correlated well ( $R^2=0.90$ ,  $P<0.01$ ).  
173 TEOM reported approximately 24% lower mass concentration than EBAM, and the difference  
174 could be explained by the loss of semi-volatile materials from TEOM (Zhu et al., 2007).

### 175 2.3 Filter sampling and chemical analysis

176 In this study, filter sampling was conducted at the five urban sites of Beijing, Guangzhou,  
177 Lhasa, Shenyang and Chongqing as well as at the six background sites of Xinglong, Lin'an,  
178 Dinghu Mountain, Namsto, Changbai Mountain and Gongga Mountain. The Automatic Cartridge  
179 Collection Unit (ACCU) system of Rupprecht & Patashnick Co. with 47 mm diameter quartz fiber  
180 filters (Pall Life Sciences, Ann Arbor, MI, USA) was deployed in Beijing to collect the  $\text{PM}_{2.5}$   
181 samplers (Liu et al., 2016a). Similar to the ACCU system, a standard 47 mm filter holder with  
182 quartz fiber filters (Pall Life Sciences, Ann Arbor, MI, USA) was placed in the bypass line of  
183 TEOM 1400a and TEOM 1405 using quick-connect fittings and was used to collect the  $\text{PM}_{2.5}$   
184 samplers of the other nine sites, excepting Guangzhou and Lin'an. Each set of the  $\text{PM}_{2.5}$  samples  
185 was continuously collected over 48 h on the same days of each week, generally starting at  
186 8:00 a.m. The flow rates were typically 15.6 L/min. For the Guangzhou site, the fine particles  
187 were collected on Whatman quartz fiber filters using an Andersen model SA235 sampler  
188 (Andersen Instruments Inc.) with an air flow rate of 1.13  $\text{m}^3/\text{min}$ . The sampling lasted 48h for the  
189 first three samples and 24 h for the rest samples, generally starting at 8:00 a.m. For the Lin'an site,  
190 a medium volume  $\text{PM}_{2.5}$  sampler (Model: TH-150CIII, Tianhong Instrument CO., Ltd. Wuhan,  
191 China) was used to collect 24 h of  $\text{PM}_{2.5}$  aerosols on 90 mm quartz fiber filters (QMA, Whatman,  
192 UK) once every 6 days (Xu et al., 2017). The sampling periods of these 11 urban and background  
193 sites are shown in Table S1.

194 All the filters were heat treated at 500  $^{\circ}\text{C}$  for at least 4 h for cleaning prior to filter sampling.  
195 The  $\text{PM}_{2.5}$  mass concentrations were obtained via the gravimetric method with an electronic  
196 balance with a detection limit of 0.01 mg (Sartorius, Germany) after stabilizing at a constant  
197 temperature ( $20\pm 1$   $^{\circ}\text{C}$ ) and humidity ( $45\%\pm 5\%$ ).  $\text{PM}_{2.5}$  mass concentrations measured by  
198 gravimetric method correlated well with the on-line instruments (TEOM and EBAM) as showed in  
199 Fig. S1b. On average,  $\text{PM}_{2.5}$  mass concentrations measured by the filter sampling was  
200 approximately 9% higher than the on-line instruments. Three types of chemical species were  
201 measured using the methods described in Xin et al. (2015). Briefly, the organic carbon (OC) and  
202 elemental carbon (EC) values were determined using a thermal/optical reflectance protocol using a  
203 DRI model 2001 carbon analyzer (Atmoslytic, Inc., Calabasas, CA, USA) with the thermal/optical  
204 reflectance (TOR) method. A circle piece of 0.495  $\text{cm}^2$  was cut off from the filters and was sent  
205 into the thermal optical carbon analyzer. In a pure helium atmosphere, OC1, OC2, OC3 and OC4  
206 are produced stepwise at 140  $^{\circ}\text{C}$ , 280  $^{\circ}\text{C}$ , 480  $^{\circ}\text{C}$  and 580  $^{\circ}\text{C}$ , respectively; followed by EC1  
207 (540  $^{\circ}\text{C}$ ), EC2 (780  $^{\circ}\text{C}$ ) and EC3 (840  $^{\circ}\text{C}$ ) in a 2% oxygen-contained helium atmosphere. Eight  
208 main ions, including  $\text{K}^+$ ,  $\text{Ca}^{2+}$ ,  $\text{Na}^+$ ,  $\text{Mg}^{2+}$ ,  $\text{NH}_4^+$ ,  $\text{SO}_4^{2-}$ ,  $\text{NO}_3^-$  and  $\text{Cl}^-$ , were measured via ion  
209 chromatography (using a Dionex DX 120 connected to a DX AS50 autosampler for anions and a  
210 DX ICS90 connected to a DX AS40 autosampler for cations). One-quarter of each filter substrate

211 was extracted with 25 mL deionized water in a PET vial for 30 min. Before performing a targeted  
212 sample analysis, a standard solution and blank test were performed, and the correlation coefficient  
213 of the standard samples was more than 0.999. The detection limits for all anions and cations, which  
214 were calculated as three times the standard deviations of seven replicate blank samples, are all lower  
215 than  $0.3 \mu\text{g m}^{-3}$  (Liu et al., 2017). The microwave acid digestion method was used to digest the filter  
216 samples into liquid solution for elemental analysis. One quarter of each filter sample was placed in  
217 the digestion vessel with a mixture of 6 mL  $\text{HNO}_3$ , 2 mL  $\text{H}_2\text{O}_2$  and 0.6 mL HF, and was then exposed  
218 to a three-stage microwave digestion procedure from a microwave-accelerated reaction system  
219 (MARS, CEM Corporation, USA). After that, 18 elements, including Mg, Al, K, Ca, V, Cr, Mn, Fe,  
220 Co, Ni, Cu, Zn, As, Se, Ag, Cd, Tl and Pb, were determined by Agilent 7500a inductively coupled  
221 plasma mass spectrometry (ICP-MS, Agilent Technologies, Tokyo, Japan). Quantification was  
222 carried out by the external calibration technique using a set of external calibration standards  
223 (Agilent Corporation) at concentration levels close to that of the samples. The relative standard  
224 deviation for each measurement (repeated twice) was within 3%. The method detection limits  
225 (MDLs) were determined by adding 3 standard deviations of the blank readings to the average  
226 blank values (Yang et al., 2009). Quality control and quality assurance procedures were routinely  
227 applied for all the carbonaceous, ion and elemental analysis.

228

### 229 3. Results and discussions

#### 230 3.1 Characteristics of $\text{PM}_{2.5}$ mass concentrations at urban and background sites

##### 231 3.1.1 Average $\text{PM}_{2.5}$ levels

232 The location, station information and average  $\text{PM}_{2.5}$  concentrations from the 40 monitoring  
233 stations are shown in Fig. 1 and Table 1. The highest  $\text{PM}_{2.5}$  concentrations were observed at the  
234 urban stations of Xi'an ( $125.8 \mu\text{g/m}^3$ ), Taiyuan ( $111.5 \mu\text{g/m}^3$ ), Ji'nan ( $107.5 \mu\text{g/m}^3$ ) and  
235 Shijiazhuang ( $105.1 \mu\text{g/m}^3$ ), which are located in the most polluted areas of the Guanzhong Plain  
236 (GZP) and the North China Plain (NCP). Several studies have revealed that the enhanced  $\text{PM}_{2.5}$   
237 pollutions of the GZP and NCP are not only due to the primary emissions from local sources such  
238 as the local industrial, domestic and agricultural sources but are also due to secondary productions  
239 (Huang et al., 2014; Guo et al., 2014; Wang et al., 2014). Furthermore, the climates of the GZP  
240 and NCP are characterized by stagnant weather with weak winds and relatively low boundary  
241 layer heights, leading to favorable atmospheric conditions for the accumulation, formation and  
242 processing of aerosols (Chan and Yao, 2008). Note that the averaged  $\text{PM}_{2.5}$  concentrations in  
243 Beijing and Tianjin were approximately  $70 \mu\text{g/m}^3$ , which is much lower than those of the other  
244 cities, including Ji'nan and Shijiazhuang in the NCP, possibly because Beijing and Tianjin are  
245 located in the northern part of the NCP, far from the intense industrial emission area that is mainly  
246 located in the southern part of the NCP. Interestingly, the average  $\text{PM}_{2.5}$  concentrations at Yucheng  
247 ( $102.8 \mu\text{g/m}^3$ ) and Xianghe ( $83.7 \mu\text{g/m}^3$ ) were even higher than most of those from the urban  
248 stations. Although Yucheng is a rural site, it is located in an area with rapid urbanization near  
249 Ji'nan and is therefore subjected to the associated large quantities of air pollutants. In addition,  
250 Xianghe is located between Beijing and Tianjin and is influenced by the regionally transported  
251 contributions from nearby megacities and the primary emissions from local sources. Yantai is a  
252 coastal city with relatively low PM concentrations compared to those of with inland cities on the

253  
254  
255  
256  
257  
258  
259  
260  
261  
262  
263  
264  
265  
266  
267  
268  
269  
270  
271  
272  
273  
274  
275  
276  
277  
278  
279  
280  
281  
282  
283  
284  
285  
286  
287  
288  
289  
290  
291  
292  
293  
294

NCP.  
The PM<sub>2.5</sub> concentrations were also high in the Yangtze River Delta (YRD), which is another developed and highly-populated city cluster area like the NCP (Fu et al., 2013). The average PM<sub>2.5</sub> values of the three urban stations of Shanghai, Wuxi and Hefei were 56.2, 65.2 and 80.4 µg/m<sup>3</sup>, respectively, which are comparable to those of the megacities of Beijing and Tianjin in the NCP. Due to the presence of fewer coal-based industries and dispersive weather conditions, the PM<sub>2.5</sub> concentrations of the Pearl River Delta (PRD) are generally lower than those of the other two largest city clusters in China, such as those from the NCP and YRD. The average PM<sub>2.5</sub> value at Guangzhou was 44.1 µg/m<sup>3</sup>, which was similar to the PM<sub>2.5</sub> values of the background stations from the NCP and YRD. Shenyang, the capital of the province of Liaoning, is located in the Northeast China Region (NECR), which is an established industrial area. High concentrations of trace gases and aerosol scattering in the free troposphere have been observed via aircraft observations and are due to regional transports and heavy local industrial emissions (Dickerson et al., 2007). In the present study, the average PM<sub>2.5</sub> concentration of Shenyang was 77.6 µg/m<sup>3</sup>. Meanwhile, Hailun, which is a rural site in northeastern China, had an average PM<sub>2.5</sub> concentration of 41.6 µg/m<sup>3</sup>, which was much lower than that of the rural site of Yucheng in the NCP.

High aerosol optical depths and low visibilities have been observed in the Sichuan Basin (Zhang et al., 2012), which is located in the Southwestern China Region (SWCR). The poor dispersion conditions and heavy local industrial emissions make this another highly polluted area in China. In the present study, the average PM<sub>2.5</sub> concentration in Chengdu was measured as 102.2 µg/m<sup>3</sup>, which is much higher than the averages from the megacities of Beijing, Shanghai and Guangzhou but is comparable to those of Ji'nan and Shijiazhuang. Chongqing, another megacity located in the SWCR, however, showed much lower PM<sub>2.5</sub> values than Chengdu. Urumqi, the capital of the Uighur Autonomous Region of Xinjiang, located in northwestern China, experiences air pollution due to its increasing consumption of fossil fuel energy and steadily growing fleet of motor vehicles (Mamtimin and Meixner, 2011). The average PM<sub>2.5</sub> concentration measured in Urumqi is 104.1 µg/m<sup>3</sup>, which is comparable to those of the urban sites in the GZP and NCP. The similarity among the PM<sub>2.5</sub> values for Cele, Dunhuang and Fukang is due to their location, being far from regions with intensive economic development but strongly affected by sandstorms and dust storms due to their proximity to dust source areas. For example, the average PM<sub>2.5</sub> concentration in Cele during the spring (200.7 µg/m<sup>3</sup>) was much greater than those of the other three seasons. Lhasa, the capital of the Tibet Autonomous Region (TAR), is located in the center of the Tibetan Plateau at a very high altitude of 3700 m. The PM<sub>2.5</sub> concentrations in Lhasa were low, with average values of 30.6 µg/m<sup>3</sup>, because of its relatively small population and few industrial emissions.

Much lower PM<sub>2.5</sub> concentrations were observed at the background stations, the values of which ranged from 11.2 to 46.5 µg/m<sup>3</sup>. The lowest concentration of PM<sub>2.5</sub> was observed in Namsto, a background station on the TAR with nearly no anthropogenic effects. The highest PM<sub>2.5</sub> concentration of the background stations was observed at Lin'an, a background station in the PRD. The average PM<sub>2.5</sub> concentration at the urban and background sites in this study are shown as box-plots in Fig. S2a. The average PM<sub>2.5</sub> concentration of the background stations (a total of 12

295 sites) is  $28.5 \mu\text{g}/\text{m}^3$ , and the average concentration of the  $\text{PM}_{2.5}$  values from urban stations (a total  
296 of 20 sites) is  $73.2 \mu\text{g}/\text{m}^3$ . The latter value is approximately three times the former, suggesting the  
297 large differences in fine particle pollution at urban and background sites across China. To further  
298 characterize these kinds of differences for different parts of China, six pairs of  $\text{PM}_{2.5}$  values  
299 measured from urban and background stations were selected to represent the NCP, YRD, PRD,  
300 TAR, NECR and SWCR, respectively (Fig. S2). The first three areas (NCP, YRD and PRD) and  
301 the last two areas (NECR and SWCR) were the most industrialized and populated regions in China,  
302 while TAR is the cleanest area in China. The  $\text{PM}_{2.5}$  concentrations of the background stations in  
303 the NCP, YRD and PRD are  $39.8 \mu\text{g}/\text{m}^3$  (Xinglong),  $46.5 \mu\text{g}/\text{m}^3$  (Lin'an) and  $40.1 \mu\text{g}/\text{m}^3$  (Dinghu  
304 Mountain) and are much higher than those of the background stations in other parts of China,  
305 which are usually below  $25 \mu\text{g}/\text{m}^3$ . All values especially for those observed in urban and rural sites  
306 in this study were much greater than the results from Europe and North America. For  
307 urban/suburban sites, average  $\text{PM}_{2.5}$  concentrations of  $20.1 \mu\text{g}/\text{m}^3$  was reported by Gehrig and  
308 Buchmann (2003) from 1998 to 2001 in Switzerland, and average concentrations of  $16.3 \mu\text{g}/\text{m}^3$  for  
309 the period 2008-2009 in the Netherlands (Janssen et al., 2013). Between October 2008 and April  
310 2011, the 20 study areas covered major cities of the European ESCAPE project showed annual  
311 average concentrations of  $\text{PM}_{2.5}$  ranging from  $8.5$  to  $29.3 \mu\text{g}/\text{m}^3$ , with low concentrations in  
312 northern Europe and high concentrations in southern and eastern Europe (Eeftens et al., 2012).  
313 Based on a constructed database of  $\text{PM}_{2.5}$  component concentrations from 187 counties in the  
314 United States for 2000-2005, Bell et al. (2007) reported an average  $\text{PM}_{2.5}$  value of  $14.0 \mu\text{g}/\text{m}^3$ ,  
315 with higher values in the eastern United States and California, and lowest values in the central  
316 regions and Northwest. For background sites, Putaud et al. (2010) showed that annual average of  
317  $\text{PM}_{2.5}$  ranged from  $3$  to  $22 \mu\text{g}/\text{m}^3$  observed from 12 background sites across Europe. In addition,  
318 average  $\text{PM}_{2.5}$  value of  $12.6 \mu\text{g}/\text{m}^3$  was observed at a regional background site in the Western  
319 Mediterranean from 2002 to 2010 (Cusack et al., 2012).

### 320 **3.1.2 Seasonal variations of $\text{PM}_{2.5}$ mass concentrations**

321 Generally, the  $\text{PM}_{2.5}$  concentrations in urban areas show distinct seasonal variabilities, with  
322 maxima during the winter and minima during the summer for most of China (Fig. 1), which is a  
323 similar pattern to that of the results reported by Zhang and Cao (2015). In northern and  
324 northeastern China, the wintertime peak values of  $\text{PM}_{2.5}$  were mainly attributed to the combustion  
325 of fossil fuels and biomass burning for domestic heating over extensive areas, which emit large  
326 quantities of primary particulates as well as the precursors of secondary particles (He et al., 2001).  
327 In addition, new particle formation and the secondary production of both inorganic aerosols and  
328 OM could further enhance fine PM abundance (Huang et al., 2014; Guo et al., 2014). Furthermore,  
329 the planetary boundary layer is relatively low in the winter, and more frequent occurrences of  
330 stagnant weather and intensive temperature inversions cause very bad diffusion conditions, which  
331 can result in the accumulation of atmospheric particulates and lead to high-concentration PM  
332 episodes (Quan et al., 2014; Zhao et al., 2013b). In southern and eastern China, although the effect  
333 of domestic heating is not as important as that in northern China, the weakened diffusion and  
334 transport of pollutants from the north due to the activity of the East Asian Winter Monsoon  
335 reinforces the pollution from large local emissions in the winter more than in any other season (Li  
336 et al., 2011; Mao et al., 2017). For northwestern and West Central China, the most polluted season

337 is the spring instead of the winter due to the increased contribution from dust particles in this  
338 desert-like region (Zou and Zhai, 2004), suggesting that the current PM<sub>2.5</sub> control strategies (i.e.,  
339 reducing fossil/non-fossil combustion derived VOCs and PM emissions) will only partly reduce  
340 the PM<sub>2.5</sub> pollution in western of China. PM<sub>2.5</sub> is greatly decreased during the summer in urban  
341 areas, which is associated with the reduced anthropogenic emissions from fossil fuel combustion  
342 and biomass burning domestic heating. Further, the more intense solar radiation causes a higher  
343 atmospheric mixing layer, which leads to strong vertical and horizontal aerosol dilution effects  
344 (Xia et al., 2006). In addition, increased precipitation in most of China due to the summer  
345 monsoon can increase the wet scavenging of atmospheric particles. As a result, PM<sub>2.5</sub> minima are  
346 observed in the summer at urban sites.

347 The seasonal variations of PM<sub>2.5</sub> at the background sites varied in different parts of China  
348 (Fig. 3). Dinghu Mountain and Lin'an showed maximum values in the winter, while Zangdongnan,  
349 Qinghai Lake, Xishuangbanna and Mount Everest showed maximum values in the spring. In  
350 addition, a summer maximum of PM<sub>2.5</sub> was observed for Xinglong, and an autumn maximum was  
351 observed for Tongyu. Changbai Mountain, Gongga Mountain and Namsto showed weak seasonal  
352 variabilities. These results suggest the different contributions from regional anthropogenic and  
353 natural emissions and long-range transports to background stations. The monthly average PM<sub>2.5</sub>  
354 concentrations of the urban and background sites in the NCP, YRD, PRD, TAR, NECR and SWCR  
355 are further analyzed and shown in Fig. 2. The monthly variations of the PM<sub>2.5</sub> concentrations at  
356 the background sites in the YRD and PRD were consistent with those of the nearby urban sites,  
357 both of which showed maximum values in December (YRD) and January (PRD). The reasons for  
358 this similarity are primarily the seasonal fluctuations of emissions, which are already well known  
359 due to the similar variations of other parameters, including sulfur dioxide and nitrogen oxide, as  
360 shown in Fig. S3. In contrast, the monthly variations of PM<sub>2.5</sub> at Xinglong showed different trends  
361 than those of the nearby urban stations. The maximum value of PM<sub>2.5</sub> at this site was observed in  
362 July, while the maximum value in Beijing was observed in January. The reasons for this are not  
363 primarily the seasonal fluctuations of emissions, but rather meteorological effects (frequent  
364 inversions during the winter and strong vertical mixing during the summer). The Xinglong site is  
365 situated at an altitude of 900 m a.s.l., and therefore, during the wintertime, the majority of cases  
366 above the inversion layer are protected from the emissions of the urban agglomerations of the NCP.  
367 Furthermore, in the NCP area, northerly winds prevail in the winter, while southerly winds prevail  
368 in the summer. Thus, in the summer, more air masses from the southern urban agglomerations will  
369 lead to high PM<sub>2.5</sub> concentrations in Xinglong. Weak monthly variabilities were observed for  
370 Namsto, Changbai Mountain and Gongga Mountain, although remarkable monthly variabilities  
371 were found at the nearby cities of Lhasa, Shenyang and Chongqing. The reasons for this difference  
372 are mainly that these three sites are elevated remote stations that are far from human activities and  
373 show predominant meteorological influences.

### 374 **3.1.3 Diurnal variations of PM<sub>2.5</sub> mass concentrations**

375 To derive importance information to identify the potential emission sources and the times  
376 when the pollution levels exceed the proposed standards, hourly data were used to examine the  
377 diurnal variabilities of PM<sub>2.5</sub> as well as those of the other major air pollutants. Fig. 3 illustrates the  
378 diurnal variations of the hourly PM<sub>2.5</sub> concentrations in Beijing, Shanghai, Guangzhou, Lhasa,

379 Shenyang and Chongqing, in the largest megacities in the NCP, YRD, PRD, TAR, NECR and  
380 SWCR and in the different climatic zones of China, respectively. Of the urban sites, Lhasa has the  
381 lowest PM<sub>2.5</sub> concentrations, but the most significant pronounced diurnal variations of PM<sub>2.5</sub>, with  
382 obvious morning and evening peaks appearing at 10:00 and 22:00 (Beijing Time) due to the  
383 contributions of enhanced anthropogenic activity during the rush hours. The minimum value  
384 occurred at 16:00, which is mainly due to a higher atmospheric mixing layer, which is beneficial  
385 for air pollution diffusion. This bimodal pattern was also observed in Shenyang and Chongqing,  
386 which show morning peaks at 7:00 and 9:00 and evening peaks at 19:00 and 20:00, respectively.  
387 However, the PM<sub>2.5</sub> values in Beijing, Shanghai and Guangzhou showed much weaker urban  
388 diurnal variation patterns, and slightly higher PM<sub>2.5</sub> concentrations during the night than during  
389 the day were observed, which can be explained by the enhanced emissions from heating and the  
390 relatively low boundary layer. **Moreover, fine particles emitted from diesel truck traffic which is**  
391 **allowed only during nighttime would additionally increase PM<sub>2.5</sub> burden because emission factors**  
392 **of heavy-duty vehicles are 6 times than those from light-duty vehicles (Westerdahl et al., 2009).**  
393 Note that the morning peaks in Beijing, Shanghai and Guangzhou were not as obvious as those of  
394 other cities, although both the SO<sub>2</sub> and NO<sub>2</sub> values increased due to increased anthropogenic  
395 emissions (Fig. S4). Alternatively, this decreasing trend may be the result of an increasing  
396 boundary layer depth. **The invisible morning peak of PM<sub>2.5</sub> in these three cities was possibly**  
397 **attributed to the stricter emission standards applied at recently years. As showed in Fig.S5, the**  
398 **morning peak of PM<sub>2.5</sub> in Beijing was gradually disappeared or invisible after National 5 vehicle**  
399 **emission standard applied at the beginning of 2013 (www.bjpc.gov.cn). The same thing would be**  
400 **also observed in Shanghai and Guangzhou which implemented the same vehicle emission**  
401 **standards followed Beijing, while it not true for the other cities as the latest vehicle emission**  
402 **standard was usually applied 2-3 years later than the three megacities.** At the urban sites of Beijing,  
403 Shanghai and Guangzhou, the PM<sub>2.5</sub> levels started to increase in the late afternoon, which could be  
404 explained by the increasing motor vehicle emissions as NO<sub>2</sub> is also dramatically increased during  
405 the same period.

406 At the background area of the TAR, significant pronounced diurnal variations of PM<sub>2.5</sub> were  
407 observed in Namsto, with a morning peak at 9:00 and an evening peak at 21:00 (Fig. 3d), which  
408 are similar to those of the urban site of Lhasa. As there are hardly any anthropogenic activities  
409 near Namsto, this kind of diurnal pattern of PM<sub>2.5</sub> may be influenced by the evolution of the  
410 planetary boundary layer. **Both Gongga Mountain and Lin'an showed the same bimodal pattern of**  
411 **PM<sub>2.5</sub> as that in Namsto, the former site could also be influenced by the planetary boundary layer,**  
412 **while the latter site was not only influenced by the evolution of the planetary boundary layer but**  
413 **also would be highly affected by the regional transportation from the YRD region.** For the  
414 background site of the NCP, however, Xinglong showed smooth PM<sub>2.5</sub> variations. As mentioned  
415 before, the Xinglong station is located on the mountain and has an altitude of 960 m a.s.l. The  
416 mixed boundary layer of the urban area increases in height in the morning and reaches a height of  
417 approximately 1000 meters in the early afternoon. Then, the air pollutants from the urban area  
418 start to affect the station as the vertical diffusion of the airflow and the PM<sub>2.5</sub> concentration reach  
419 their maxima at 18:00. Next, the concentration starts to decrease when the mixed boundary layer  
420 collapses in the late afternoon, eventually forming the nocturnal boundary layer (Boyouk et al.,

421 2010). Thus, PM<sub>2.5</sub> concentration decreased slowly during the night and morning, reaching a  
422 minimum at 10:00. At Dinghu Mountain and Changbai Mountain, the daytime PM<sub>2.5</sub> greater than  
423 that of the nighttime, with a maximum value occurring at approximately 11:00-12:00. This kind of  
424 diurnal pattern of PM<sub>2.5</sub> is mainly determined by the effects of the mountain-valley breeze. Both  
425 the Dinghu Mountain and Changbai Mountain stations are located near the mountain. Thus, during  
426 daytime, the valley breeze from urban areas carries air pollutants that will accumulate in front of  
427 the mountain and cause an increase of the PM concentration. Meanwhile, at night, the fresh air  
428 carried by the mountain breeze will lead to the dilution of the PM, so low concentrations are  
429 sustained during the night. Further support for this pattern comes from the much higher maximum  
430 values of PM<sub>2.5</sub> in the winter than those in the summer, as enhanced air pollutant emissions in  
431 urban areas are expected in the winter due to heating.

### 432 3.2 Chemical compositions of PM<sub>2.5</sub> in urban and background sites

#### 433 3.2.1 Overview of PM<sub>2.5</sub> mass speciation

434 Figure 4 shows the annual average and seasonal average chemical compositions of PM<sub>2.5</sub> at  
435 six urban and six background sites, which represent the largest megacities and regional  
436 background areas of the NCP, YRD, PRD, TAR, NECR and SWCR. The chemical species of  
437 PM<sub>2.5</sub> in Shanghai were obtained from Zhao et al. (2015). The atmospheric concentrations of the  
438 main PM<sub>2.5</sub> constituents are also shown in Table 2. The EC, nitrate (NO<sub>3</sub><sup>-</sup>), sulfate (SO<sub>4</sub><sup>2-</sup>),  
439 ammonium (NH<sub>4</sub><sup>+</sup>) and chlorine (Cl<sup>-</sup>) concentrations were derived directly from measurements.  
440 Organic matter (OM) was calculated assuming an average molecular weight per carbon weight,  
441 showing an OC of 1.6 at the urban sites and of 2.1 at the background sites, based on the work of  
442 Turpin and Lim (2001); however, these values are also spatially and temporally variable, and  
443 typical values could range from 1.3 to 2.16 (Xing, et al., 2013). The calculation of mineral dust  
444 was performed on the basis of crustal element oxides (Al<sub>2</sub>O<sub>3</sub>, SiO<sub>2</sub>, CaO, Fe<sub>2</sub>O<sub>3</sub>, MnO<sub>2</sub> and K<sub>2</sub>O).  
445 In addition, the Si content, which was not measured in this study, was calculated based on its ratio  
446 to Al in crustal materials (Mason, 1966); namely, [Si]=3.41×[Al]. Finally, the unaccounted-for  
447 mass refers to the difference between the PM<sub>2.5</sub> gravimetric mass and the sum of the PM  
448 constituents mentioned above.

449 The PM constituents' relative contributions to the PM mass are independent of their  
450 dilutions and reflect differences in the sources and processes controlling the aerosol compositions  
451 (Putaud et al., 2010). When all the main aerosol components except water are quantified, they  
452 account for 73.6-84.8% of the PM<sub>2.5</sub> mass (average 79.2%) at urban sites and for 76.2-91.1% of  
453 the PM<sub>2.5</sub> mass (average 83.4%) at background sites. The remaining unaccounted-for mass fraction  
454 may be the result of analytical errors, a systematic underestimation of the PM constituents whose  
455 concentrations are calculated from the measured data (e.g., OM, and mineral dust), and  
456 aerosol-bound water (especially when mass concentrations are determined at RH >30%). For the  
457 urban sites, the mean composition given in descending concentrations is 26.0% OM, 17.7% SO<sub>4</sub><sup>2-</sup>,  
458 11.8% mineral dust, 9.8% NO<sub>3</sub><sup>-</sup>, 6.6% NH<sub>4</sub><sup>+</sup>, 6.0% EC and 1.2% Cl<sup>-</sup>. For the background sites, the  
459 mean composition given in descending concentrations is 33.2% OM, 17.8% SO<sub>4</sub><sup>2-</sup>, 10.1% mineral  
460 dust, 8.7% NH<sub>4</sub><sup>+</sup>, 8.6% NO<sub>3</sub><sup>-</sup>, 4.1% EC and 0.9% Cl<sup>-</sup>. Generally, the chemical compositions of the  
461 PM<sub>2.5</sub> at background sites are similar to those of the urban sites, although they show a much higher  
462 fraction of OM and lower fractions of NO<sub>3</sub><sup>-</sup> and EC. Significant seasonal variations of the

463 chemical compositions were observed at urban sites (Fig. 4c), with much higher fractions of OM  
464 (33.7%) and  $\text{NO}_3^-$  (11.1%) in the winter and much lower fractions of OM (20.7%) and  $\text{NO}_3^-$  (6.9%)  
465 in the summer. In contrast, the fraction of  $\text{SO}_4^{2-}$  was consistent among the different seasons,  
466 although its absolute concentration in the winter ( $14.9 \mu\text{g}/\text{m}^3$ ) was higher than that in the summer  
467 ( $11.7 \mu\text{g}/\text{m}^3$ ). Compared with those at urban sites, different seasonal variation of OM were  
468 observed at the background sites, which showed summer maxima and winter/spring minima (Fig.  
469 4d). While the wintertime peaks of OM at the urban sites were probably due to additional local  
470 emissions sources related to processes like heating, the summer peaks at the background sites were  
471 attributed to the enhanced biogenic emissions. Note that the seasonal variations of  $\text{NO}_3^-$  were  
472 similar to those at urban sites; this seasonal phenomenon is due to the favorable conditions of cold  
473 temperature and high relative humidity conditions leading to the formation of particulate nitrate.  
474 The seasonal behaviors of  $\text{SO}_4^{2-}$  at the background sites were markedly different than those of the  
475 urban sites and indicate very different sources and atmospheric processing of  $\text{SO}_4^{2-}$ , which will be  
476 further discussed for specific regions of China.

477 There are significant variations of the absolute speciation concentrations at these urban and  
478 background sites (Table 2). For the urban sites, the OM concentrations span a 2-fold concentration  
479 range from  $12.6 \mu\text{g}/\text{m}^3$  (Lhasa) to  $23.3 \mu\text{g}/\text{m}^3$  (Shenyang), while these values range from  $3.4$   
480  $\mu\text{g}/\text{m}^3$  (Namtso) to  $21.7 \mu\text{g}/\text{m}^3$  (Lin'an) at the background sites. The  $\text{SO}_4^{2-}$  and  $\text{NO}_3^-$  concentrations  
481 exhibit larger spatial heterogeneities than those of the OM for both urban and background sites.  
482 The absolute values of  $\text{SO}_4^{2-}$  have an approximately 25-fold range in urban sites, from  $0.8 \mu\text{g}/\text{m}^3$   
483 (Lhasa) to  $19.7 \mu\text{g}/\text{m}^3$  (Chongqing), while this value has a 30-fold range at the background sites,  
484 from  $0.4 \mu\text{g}/\text{m}^3$  (Namtso) to  $11.2 \mu\text{g}/\text{m}^3$  (Lin'an). The corresponding mass fractions are 26.8% in  
485 Chongqing and below 3% in Lhasa. Much higher fractions of  $\text{SO}_4^{2-}$  in the  $\text{PM}_{2.5}$  were observed at  
486 the urban sites located in southern China than those in northern China, although the average  
487 concentration of  $\text{PM}_{2.5}$  is greater in the north than in the south, suggesting that sulfur pollution  
488 remains a problem for southern China (Liu, et al., 2016b). This problem may be attributed to  
489 higher sulfur contents of the coal in southern China, with 0.51% in the north vs. 1.32% in the  
490 south and up to >3.5% in Chongqing in southern China (Lu et al., 2010; Zhang et al., 2010). **In**  
491 **addition, the higher fraction of sulfate in south China is also likely associated to the higher oxidation**  
492 **capacity in south China and therefore higher formation efficiency from  $\text{SO}_2$  to  $\text{SO}_4^{2-}$ .** The absolute  
493 values of  $\text{NO}_3^-$  have an approximately 20-fold range in urban sites and a greater than 100-fold  
494 range in background sites. This heterogeneity reflects the large spatial and temporal variations of  
495 the  $\text{NO}_x$  sources. For the urban sites, the absolute EC values have a 5-fold concentration range,  
496 from  $1.4 \mu\text{g}/\text{m}^3$  (Lhasa) to greater than  $7.0 \mu\text{g}/\text{m}^3$  (Guangzhou), while this species has a 15-fold  
497 concentration range at the background sites and is mainly from anthropogenic sources. In  
498 comparison, the absolute concentrations of mineral dust exhibit much weaker spatial variations at  
499 the urban and background sites.

500 The characteristics of the  $\text{PM}_{2.5}$  chemical compositions at individual site were discussed in  
501 more detail. In this section, six pairs of urban and background sites from each region of China  
502 were selected, and the differences in the chemical compositions of urban and background sites  
503 were analyzed.

### 504 3.2.2 North China Plain

505 Beijing is the capital of China and has attracted considerable attention due to its air pollution  
506 (Chen et al., 2013). Beijing is the largest megacity in the NCP, which is surrounded by the  
507 Yanshan Mountains to the west, north and northeast and is connected to the Great North China  
508 Plain to the south. The filter sampler is located in the courtyard of the Institute of Atmospheric  
509 Physics (IAP) (116.37°E, 39.97°N), 8 km northwest of the center of downtown. The PM<sub>2.5</sub>  
510 concentration during the filter sampling period was 71.7 µg/m<sup>3</sup>, which is close to the three-year  
511 average PM<sub>2.5</sub> value reported by TEOM (Table 1). PM<sub>2.5</sub> in Beijing is mainly composed by OM  
512 (26.6%), SO<sub>4</sub><sup>2-</sup> (16.5%) and NO<sub>3</sub><sup>-</sup> (13.0%) (Fig. 5a), which compare well with previous studies  
513 (Yang et al., 2011; Oanh et al., 2006). However, the mineral dust fraction found in this study  
514 (6.5%) was much lower than that found in Yang et al. (2011) (19%) but was comparable to that  
515 found in Oanh et al. (2006) (5%), potentially due to difference in definitions. **In addition, the EC**  
516 **fraction (5.7%) was slightly lower than those found in previous studies (7%-7.4%) (Yang et al.,**  
517 **2011; Wang et al., 2015a).** The annual concentration of OM (19.1 µg/m<sup>3</sup>) in Beijing was  
518 comparable to those in Shanghai, Guangzhou and Chongqing, but was much lower than that in  
519 Shenyang. Higher fractions of OM were observed in the winter (34.2%) and autumn (30.5%) than  
520 in the summer (21.6%) and spring (20.9%). The annual concentration of SO<sub>4</sub><sup>2-</sup> (11.9 µg/m<sup>3</sup>) was  
521 much lower than those of earlier years (15.8 µg/m<sup>3</sup>, 2005-2006) (Yang et al., 2011), suggesting  
522 that the energy structure adjustment implemented in Beijing (e.g., replacing coal fuel with natural  
523 gas) has been effective in decreasing the particulate sulfate in Beijing. Further support for this  
524 comes from the SO<sub>4</sub><sup>2-</sup> concentration in the winter (16.5 µg/m<sup>3</sup>) being comparable to that in the  
525 summer (13.4 µg/m<sup>3</sup>). The significant NO<sub>3</sub><sup>-</sup> value (9.3 µg/m<sup>3</sup>) reflects the significant urban NO<sub>x</sub>  
526 emissions in Beijing, which was greatest during the winter, as expected from ammonium-nitrate  
527 thermodynamics. The greater mineral component in the spring reflects the regional natural dust  
528 sources.

529 The filter sampling site in Xinglong (117.58°E, 40.39°N) was located at Xinglong  
530 Observatory, National Astronomical Observatory, Chinese Academy of Sciences, which is 110 km  
531 northeast of Beijing (Fig. 1). This site is surrounded by mountains and is minimally affected by  
532 anthropogenic activities. The PM<sub>2.5</sub> concentration during the filter sampling period was 42.6 µg/m<sup>3</sup>,  
533 which is close to the three-year average PM<sub>2.5</sub> values reported by TEOM (Table 1). The annual  
534 chemical composition of the PM<sub>2.5</sub> in Xinglong was similar to that in Beijing, although relatively  
535 higher fractions of OM and sulfate were observed in Xinglong (Fig. 5a). Higher fractions of OM  
536 were found in the winter (36.7%), and higher fractions of sulfate were found in the summer  
537 (32.1%) than in any other season (OM: 23.0-30.4%; SO<sub>4</sub><sup>2-</sup>: 15.7-20.1%). Interestingly, the summer  
538 SO<sub>4</sub><sup>2-</sup> concentration in Xinglong (14.4 µg/m<sup>3</sup>) was even higher than that in Beijing, suggesting  
539 spatially uniform distributions of SO<sub>4</sub><sup>2-</sup> concentrations across the NCP. This result indicates that  
540 regional transport can be an important source of SO<sub>4</sub><sup>2-</sup> aerosols in Beijing, especially during the  
541 summer.

### 542 **3.2.3 Yangtze River Delta**

543 Shanghai is the economic center of China, lying on the edge of the broad flat alluvial plain of  
544 the YRD, with a few mountains to the southwest. The filter sampler was located at the top of a  
545 four-floor building of the East China University of Science and Technology (121.52°E, 31.15°N)  
546 (Zhao et al., 2015), approximately 10 km northwest of the center of downtown. The PM<sub>2.5</sub>

547 concentration during the filter sampling period was  $68.4 \mu\text{g}/\text{m}^3$ , which is greater than the  
548 three-year average  $\text{PM}_{2.5}$  value reported by EBAM, likely due to the different sampling period  
549 (Table S1). The  $\text{PM}_{2.5}$  in Shanghai mainly comprises OM (24.9%),  $\text{SO}_4^{2-}$  (19.9%) and  $\text{NO}_3^-$   
550 (17.4%), which is comparable to the results of previous studies (Ye et al., 2003; Wang et al., 2016).  
551 This site had the highest  $\text{NO}_3^-$  ( $11.9 \mu\text{g}/\text{m}^3$ ) and the second-highest  $\text{SO}_4^{2-}$  ( $13.6 \mu\text{g}/\text{m}^3$ ) values of  
552 the urban sites, while its OM ( $17.1 \mu\text{g}/\text{m}^3$ ) was comparable to those of Guangzhou and Chongqing.  
553 The  $\text{SO}_4^{2-}$  and  $\text{NO}_3^-$  values were highest during the autumn as expected based on the widespread  
554 biomass burning in the autumn in the YRD (Niu et al., 2013). However, the OM values were  
555 highest during the winter and mainly originated from secondary aerosol processes based on the  
556 highest OC/EC ratios (6.0) and the poor relationship of the OC and EC in this season.

557 Filter sampling was conducted at the Lin'an Regional Atmospheric Background Station  
558 ( $119.73^\circ\text{E}$ ,  $30.30^\circ\text{N}$ ), which is a background monitoring station for the World Meteorological  
559 Organization (WMO) global atmospheric observation network. The Lin'an site was located at the  
560 outskirts of Lin'an County within Hangzhou Municipality, which was 200 km southwest of  
561 Shanghai (Fig. 1). This site is surrounded by agricultural fields and woods and is less affected by  
562 urban, industrial and vehicular emissions (Xu et al., 2017). The  $\text{PM}_{2.5}$  concentration during the  
563 filter sampling period was  $66.3 \mu\text{g}/\text{m}^3$ , which is higher than the three-year average  $\text{PM}_{2.5}$  values  
564 reported by TEOM, likely due to the different sampling period (Table S1). The annual chemical  
565 composition of the  $\text{PM}_{2.5}$  in Lin'an was different than that in Shanghai, with much higher fractions  
566 of OM (32.7%) and  $\text{NH}_4^+$  (11.0%). Furthermore, the absolute concentration of OM in Lin'an was  
567 much higher than that in Shanghai, especially in the summer ( $21.7$  vs.  $9.9 \mu\text{g}/\text{m}^3$ ), which may be  
568 attributed to the enhanced biomass burning at both local and regional scales as well as the higher  
569 concentration of summer EC in Lin'an than in Shanghai ( $2.2$  vs.  $1.4 \mu\text{g}/\text{m}^3$ ). In addition, the  $\text{SO}_4^{2-}$   
570 and  $\text{NO}_3^-$  concentrations in Lin'an were comparable to those in Shanghai. These results suggest a  
571 spatially homogeneous distribution of secondary aerosols over the PRD and the transportation  
572 of aged aerosol and gas pollutants from city clusters has significantly changed the aerosol  
573 chemistry in the background area of this region.

### 574 3.2.4 Pearl River Delta

575 Guangzhou is the biggest megacity in south China located in the PRD and mainly consists of  
576 floodplains within the transitional zone of the East Asian monsoon system (Yang et al., 2011). The  
577 filter sampler was set up on the rooftop of a 15-m high building of the Guangzhou Institute of  
578 Geochemistry, Chinese Academy of Sciences ( $113.35^\circ\text{E}$ ,  $23.12^\circ\text{N}$ ). This site was surrounded by  
579 heavily trafficked roads and dense residential areas, representing a typical urban location. The  
580  $\text{PM}_{2.5}$  concentration during the filter sampling period was  $75.3 \mu\text{g}/\text{m}^3$ , which is much higher than  
581 the three-year average  $\text{PM}_{2.5}$  value reported by EBAM (Table 1), likely due to the different  
582 sampling period and location. The  $\text{PM}_{2.5}$  in Guangzhou mainly comprises OM (22.2%),  $\text{SO}_4^{2-}$   
583 (17.3%) and mineral dust (9.7%), which have values comparable to previous studies conducted in  
584 the years of 2013-2014 (Chen et al., 2016; Tao et al., 2017). This site has the lowest OC/EC ratio  
585 (1.5) of all urban sites, which can be explained by the abundance of diesel engine truck in  
586 Guangzhou City (Verma et al., 2010). Obvious seasonal variations of OM,  $\text{SO}_4^{2-}$  and  $\text{NO}_3^-$  were  
587 observed, showing winter/autumn maxima and summer/spring minima. In addition, summer  
588 minima were also observed for EC and  $\text{NH}_4^+$ . High mixing heights in the summer and clean air

589 masses affected by summer monsoons from the South China Sea should lead to the minima of  
590 these species in summer, while the low wind speeds, weak solar radiation, relatively low  
591 precipitation (Tao et al., 2014) and relatively high emissions (Zheng et al., 2009) result in the  
592 much higher concentrations of OM and secondary inorganic aerosols ( $\text{SO}_4^{2-}$ ,  $\text{NO}_3^-$  and  $\text{NH}_4^+$ ) in  
593 the winter and autumn.

594 Filter sampling was conducted at Dinghu Mountain Station (112.50°E, 23.15°N), which is  
595 located in the middle of Guangdong Province in southern China. This site was surrounded by hills  
596 and valleys, being approximately 70 km west of Guangzhou (Fig. 1). The  $\text{PM}_{2.5}$  concentration  
597 during the filter sampling period was  $40.1 \mu\text{g}/\text{m}^3$ , close to the three-year average  $\text{PM}_{2.5}$  values  
598 reported by TEOM. Distinct seasonal variations of OM,  $\text{SO}_4^{2-}$ ,  $\text{NO}_3^-$  and  $\text{NH}_4^+$  were observed,  
599 with the highest concentration of OM and  $\text{NO}_3^-$  occurring in the winter, while the highest  
600 concentrations of  $\text{SO}_4^{2-}$  and  $\text{NH}_4^+$  occurred in the autumn. In contrast, EC and mineral dust showed  
601 weak seasonal variations. Dinghu Mountain has the second-highest EC and  $\text{SO}_4^{2-}$  values of the  
602 background sites, being  $2.0 \mu\text{g}/\text{m}^3$  and  $10.1 \mu\text{g}/\text{m}^3$ . In addition, the lowest OC/EC ratio was  
603 observed at Dinghu Mountain (2.8); the other background sites had values ranging from 3.5-8.3.  
604 These results indicate that this background site is intensely influenced by vehicular traffic, fossil  
605 fuel combustion and industrial emissions due to the advanced urban agglomeration in the PRD  
606 region. These results are consistent with the finds from previous studies (Liu et al., 2011; Wu et al.,  
607 2016). Compared with those from Guangzhou, higher fractions of  $\text{SO}_4^{2-}$  and  $\text{NO}_3^-$  were observed  
608 at Dinghu Mountain, while the fractions of OM and mineral dust were similar at these two sites,  
609 possibly indicating that there was a significantly larger fraction of transported secondary aerosols  
610 or aged aerosols at the background site of the PRD.

### 611 3.2.5 Tibetan Autonomous Region

612 Located in the inland TAR, Lhasa is one of the highest cities in the world (at an altitude of  
613 3700 m). The city of Lhasa is located in a narrow west-east oriented valley in the southern part of  
614 the TAR. The filter sampler was located on the roof of a 20-m high building on the campus of the  
615 Institute of Tibetan Plateau Research (Lhasa branch) (91.63°E, 29.63°N). This site is close to  
616 Jinzhu road, one of the busiest roads in the city (Cong et al., 2011). The  $\text{PM}_{2.5}$  concentration  
617 during the filter sampling period was  $36.4 \mu\text{g}/\text{m}^3$ , which is close to the three-year average  $\text{PM}_{2.5}$   
618 values reported by TEOM. The  $\text{PM}_{2.5}$  in Lhasa mainly comprises OM (34.5%) and mineral dust  
619 (31.9%), and the secondary inorganic aerosols ( $\text{SO}_4^{2-}$ ,  $\text{NO}_3^-$  and  $\text{NH}_4^+$ ) contributed little to the  
620  $\text{PM}_{2.5}$  (<5%). These results are comparable to those of a previous study conducted in the year of  
621 2013-2014 (Wan et al., 2016). In addition, this site reports the lowest OM ( $12.6 \mu\text{g}/\text{m}^3$ ), secondary  
622 inorganic aerosols ( $1.7 \mu\text{g}/\text{m}^3$ ) and EC ( $1.4 \mu\text{g}/\text{m}^3$ ) values of the urban sites in this study. Higher  
623 fractions of OM were observed in the winter (48.4%) and spring (43.1%), exceeding those in the  
624 summer (24.6%) and autumn (31.2%). Weak seasonal variations were found for the  $\text{SO}_4^{2-}$   
625 (1.5-3.0%) and  $\text{NO}_3^-$  (1.1-1.7%) values, suggesting the negligible contributions from fossil fuel  
626 combustion in Lhasa.

627 Filter sampling was conducted at the Namtso Monitoring and Research Station for  
628 Multisphere Interactions (90.98°E, 30.77°N), a remote site located on the northern slope of the  
629 Nyainqen-tanglha Mountains, approximately 125 km northwest of Lhasa (Fig. 1). The  $\text{PM}_{2.5}$   
630 concentration during the filter sampling period was  $9.5 \mu\text{g}/\text{m}^3$ , which is close to the three-year

631 average PM<sub>2.5</sub> value reported by TEOM. The PM<sub>2.5</sub> in Namtso mainly comprises mineral dust  
632 (40.8%) and OM (36.3%), while SO<sub>4</sub><sup>2-</sup> and NO<sub>3</sub><sup>-</sup> contributed less than 5% to the PM<sub>2.5</sub>. This  
633 chemical composition is distinctly different from those of the other background sites in this study,  
634 but is comparable to the background site at Qinghai Lake in the TAR (Zhang et al., 2014b).  
635 Namtso has the lowest OM, EC, SO<sub>4</sub><sup>2-</sup>, NO<sub>3</sub><sup>-</sup> and NH<sub>4</sub><sup>+</sup> values of all the background sites in this  
636 study. Spring maxima and winter minima were observed for the OM and EC, while the SO<sub>4</sub><sup>2-</sup>,  
637 NO<sub>3</sub><sup>-</sup> and NH<sub>4</sub><sup>+</sup> values showed weak seasonal variations. The highest OC/EC ratio was observed  
638 (8.3) at this site, suggesting that the organic aerosols at Namtso mainly originated from secondary  
639 aerosol processes or aged organic aerosols from regional transports.

### 640 3.2.6 Northeast China Region

641 Shenyang is the capital city of Liaoning province and the largest city in northeastern China.  
642 The main urban area is located on a delta to the north of the Hun River. The filter sampler was  
643 located at the Shenyang Ecological Experimental Station of the Chinese Academy of Science  
644 (123.40°E, 41.50°N) and was surrounded by residential areas with no obvious industrial pollution  
645 sources around the monitoring station, representing the urban area of Shenyang. The PM<sub>2.5</sub>  
646 concentration during the filter sampling period was 81.8 µg/m<sup>3</sup>, which is close to the three-year  
647 average PM<sub>2.5</sub> value reported by TEOM (Table 1). The PM<sub>2.5</sub> in Shenyang mainly comprises OM  
648 (28.5%), SO<sub>4</sub><sup>2-</sup> (16.1%) and mineral dust (11.3%). This site reports the highest OM (23.3 µg/m<sup>3</sup>)  
649 and mineral dust (9.2 µg/m<sup>3</sup>) values as well as the second-highest EC (5.2 µg/m<sup>3</sup>) value of the  
650 urban sites. The NO<sub>3</sub><sup>-</sup> concentration at this site, however, was the second-lowest of the urban sites  
651 (Table 2). Much higher fractions of OM were observed in the winter (40.5%) than in the other  
652 seasons (15.6-26.5%) (Fig. 5), possibly due to the enhanced coal burning for winter heating.  
653 Further support for this pattern comes from the high abundance of chlorine during the cold seasons,  
654 which is mainly associated with coal combustion. The contribution from sea-salt particles is not  
655 important since the sampling sites are at least 200 km from the sea. Note that the fraction of SO<sub>4</sub><sup>2-</sup>  
656 in the PM<sub>2.5</sub> during the winter was lower than that in the summer, although the absolute  
657 concentration was much higher in the winter (23.6 µg/m<sup>3</sup>) than in the summer (11.3 µg/m<sup>3</sup>). This  
658 result may be attributed to the reduced transformation of sulfur dioxide at low temperatures.

659 Filter sampling was conducted at the Changbai Mountain forest ecosystem station  
660 (128.01°E, 42.40°N), which was mostly surrounded by hills and forest and is located  
661 approximately 390 km northeast of Shenyang (Fig. 1). This site is situated 10 km from the nearest  
662 town, Erdaobaihe, which has approximately 45000 residents. The sources of PM were expected to  
663 be non-local. Hence, this site is considered a background site in the NECR. The PM<sub>2.5</sub>  
664 concentration during the filter sampling period was 23.3 µg/m<sup>3</sup>, which is close to the three-year  
665 average PM<sub>2.5</sub> value reported by TEOM (Table 1). The main contributions to the PM<sub>2.5</sub> at  
666 Changbai Mountain were OM (38.1%), mineral dust (16.0%) and SO<sub>4</sub><sup>2-</sup> (14.3%), similar to those  
667 in Shenyang. Note that the summer OM concentrations were quite similar at these two sites (8.0 vs.  
668 9.0 µg/m<sup>3</sup>), but the OC/EC ratios were different (4.8 vs. 1.6), which may reflect the different  
669 origins of the OM at the urban (primary emissions) and background sites (secondary processes) of  
670 the NECR. The OM concentrations in the other seasons were much lower at Changbai Mountain  
671 than those from Shenyang city, especially during the winter (10.8 vs. 59.4 µg/m<sup>3</sup>). In fact, weak  
672 seasonal variations of chemical species (OM, EC, SO<sub>4</sub><sup>2-</sup>, NO<sub>3</sub><sup>-</sup> and NH<sub>4</sub><sup>+</sup>) were observed at

673 Changbai Mountain. This site reports the second-lowest values of OM, EC,  $\text{SO}_4^{2-}$  and  $\text{Cl}^-$  of the  
674 background sites. These results suggest that aerosols at Changbai Mountain were influenced by  
675 the regional transports alone.

### 676 **3.2.7 Southwestern China Region**

677 Chongqing is the fourth municipality near Central China, lying on the Yangtze River in  
678 mountainous southwestern China, near the eastern border of the Sichuan Basin and the western  
679 border of Central China. For topographic reasons, Chongqing has some of the lowest wind speeds  
680 in China (annual averages of 0.9-1.6  $\text{m s}^{-1}$  from 1979 to 2007; Chongqing Municipal Bureau of  
681 Statistics, 2008), which favors the accumulation of pollutants. The filter sampler was located on  
682 the rooftop of a 15-m high building on the campus of the Southwest University (106.54°E,  
683 29.59°N). This site is located in an urban district of Chongqing with no obvious industrial  
684 pollution sources around the monitoring site, representing the urban area of Chongqing. The  $\text{PM}_{2.5}$   
685 concentration during the filter sampling period was 73.5  $\mu\text{g}/\text{m}^3$ , of which 26.8% is  $\text{SO}_4^{2-}$ , 23.5%  
686 OM, 10.0% mineral dust, 8.9%  $\text{NO}_3^-$ , 8.2% EC and 6.5%  $\text{NH}_4^+$ . The OM fraction is smaller than  
687 those measured by Yang et al. (2011) (32.7%) and Chen et al., 2017 (30.8%), while the  $\text{SO}_4^{2-}$   
688 fraction is greater than the values reported in these two studies (19.8-23.0%). This site shows the  
689 highest  $\text{SO}_4^{2-}$  (19.7  $\mu\text{g}/\text{m}^3$ ), the highest  $\text{NH}_4^+$  (6.1  $\mu\text{g}/\text{m}^3$ ) and the third-highest EC (4.8  $\mu\text{g}/\text{m}^3$ )  
690 values of the urban sites. A weak seasonal variation in the chemical composition of  $\text{PM}_{2.5}$  was  
691 observed, although a much higher concentration of this species was found in the winter than in the  
692 other seasons.

693 Filter sampling was performed at the Gongga Mountain Forest Ecosystem Research Station  
694 (101.98°E, 29.51°N) in the Hailuoguo Scenic Area, a remote site located in southeastern Ganzi in  
695 the Tibetan Autonomous Prefecture in Sichuan province. This site is mostly surrounded by glaciers  
696 and forests and is located approximately 450 km northwest of Chongqing (Fig. 1). The  $\text{PM}_{2.5}$   
697 concentration during the filter sampling period was 32.2  $\mu\text{g}/\text{m}^3$ , close to the three-year average  
698  $\text{PM}_{2.5}$  value reported by TEOM (Table 1). The dominant components of  $\text{PM}_{2.5}$  were OM (40.7%),  
699  $\text{SO}_4^{2-}$  (14.6%) and mineral dust (9.8%), similar to those at Changbai Mountain. This site has the  
700 second-highest OM (13.1  $\mu\text{g}/\text{m}^3$ ) value of the background sites, which may mainly be due to  
701 secondary processes, considering the high OC/EC ratio (5.6). In addition, distinct seasonal  
702 variations of OM were observed, which shows summer maxima (19.9  $\mu\text{g}/\text{m}^3$ ) and autumn minima  
703 (9.1  $\mu\text{g}/\text{m}^3$ ). Previous studies showed higher mixing ratios of the VOCs during the spring and  
704 summer and lower mixing ratios during the autumn at Gongga Mountain (Zhang et al., 2014c),  
705 which may result in high concentrations of OM in the summer because the OC/EC ratio reaches its  
706 highest value in the summer (10.3). Second-lowest EC and  $\text{NO}_3^-$  values of the background sites  
707 were observed here, suggesting the insignificant influence of human activities in this region.

### 708 **3.3 Temporal evolution and chemical composition $\text{PM}_{2.5}$ in polluted days**

#### 709 **3.3.1 Temporal evolution of $\text{PM}_{2.5}$ mass concentration in polluted days**

710 Using the “Ambient Air Quality Standard” (GB3095-2012) of China (CAAQS), the  
711 occurrences of polluted days exceeding the daily threshold values during 2012-2014 were counted  
712 for each site (Fig. 6). Based on the number of polluted days exceeding the CAAQS daily guideline  
713 of 35  $\mu\text{g}/\text{m}^3$ , substandard days of  $\text{PM}_{2.5}$  account for more than 60% of the total period at the  
714 majority of urban sites, excepting Lhasa, Taipei and Sanya. Note that the ten most polluted cities

715 (Ji'nan, Chengdu, Taiyuan, Hefei, Shenyang, Xi'an, Changsha, Shijiazhuang, Wuxi and Chongqing)  
716 experienced less than 20% clean days (daily  $PM_{2.5} < 35 \mu g/m^3$ ) during the three-year observation  
717 period. Interestingly, the occurrences of heavily polluted days (daily  $PM_{2.5} > 150 \mu g/m^3$ ) were  
718 different among these ten most polluted cities. While more than 15% of the total period comprised  
719 heavily polluted days in Ji'nan, Taiyuan, Chengdu, Xi'an and Shijiazhuang, heavily polluted days  
720 accounted for less than 5% of the total days in the other five cities, which mainly experienced  
721 slightly polluted ( $35-75 \mu g/m^3$ ) and moderately polluted ( $75-115 \mu g/m^3$ ) days. Due to the regional  
722 pollutant transports, the rural and background sites near the most polluted cities also showed high  
723 occurrences of polluted days. Polluted days accounted for more than 50% of the total period at  
724 Xin'long, Lin'an and Dinghu Mountain. In addition, an even higher occurrence of polluted days  
725 ( $>80\%$ ) was found for the rural areas of Yucheng and Xianghe. In contrast, the background sites in  
726 the TAR, NECR and SWCR rarely experienced polluted days, and over 80% of the total period  
727 comprised clean days at these sites.

728 The polluted days were not equally distributed throughout the year. The monthly distributions  
729 for the polluted days at each site are shown in Fig. 7. In terms of the occurrences of heavily  
730 polluted days, December, January and February were predominant months for the urban sites  
731 located in the most polluted areas of the GZP and NCP, where both the unfavorable dispersion  
732 conditions for pollutants and the additional emission enhancements from residential heating  
733 contributed to the heavy pollution in the winter. The heavy pollution occurring in April and  
734 November in Cele was primarily caused by sandstorms and dust storms. Heavily polluted days  
735 were rarely observed at the 12 background sites in this study. The moderately polluted and polluted  
736 days were still mainly concentrated in the winter in the megacities of the GZP and NCP and also  
737 occurred in the winter in the megacities of the YRD and SWCR. In addition, March to June and  
738 September to October were periods with high occurrences of polluted days. Dust storms from  
739 northern China (March to April), biomass burning after crop harvests (May to June and September  
740 to October) and worsening dispersion conditions after the summers likely accounted for the  
741 polluted days (Cheng et al., 2014; Fu et al., 2014). The majority of slightly polluted days occurred  
742 from June to September, except at several urban sites in southern China. The mass level of  $35-75$   
743  $\mu g/m^3$  was considered a low level of pollution for the entire year, illustrating that the summer and  
744 early autumn experienced cleaner conditions.

### 745 3.3.2 Chemical evolution of $PM_{2.5}$ composition in polluted days

746 The mean percentile compositions of the major components in  $PM_{2.5}$  at different pollution  
747 levels from four paired urban-background sites are shown in Fig. 8. With the pollution level  
748 increased from clean to moderately polluted, the EC fraction in Beijing decreased slightly, the OM  
749 fraction decreased significantly, and the sulfate and nitrate contributions increased sharply (Fig.  
750 8a). The same chemical evolution of the  $PM_{2.5}$  was also observed at the background site of  
751 Xinglong, suggesting that regional transport plays a vital role in the formation of the slightly and  
752 moderately polluted days in the NCP. When the pollution level increased to heavily polluted,  
753 however, the OM fraction further increased and was accompanied by increases of the sulfate and  
754 nitrate contributions as well as decreases of the mineral dust contribution, indicating the enhanced  
755 secondary transformation of gaseous pollutants (etc.  $SO_2$ ,  $NO_x$ , VOCs) during heavily polluted  
756 periods (Liu et al., 2016a). **Note that a steady increase of  $[NO_3^-]/[SO_4^{2-}]$  ratio was observed with**

757 the aggravation of pollution (Fig. 8a), suggesting the relatively more important contribution of  
758 mobile than stationary sources (Arimoto et al., 1996). In addition, much higher OC/EC ratios were  
759 found in Beijing, especially during the heavily polluted days (OC/EC=6.3) (Fig. 8), compared  
760 with Guangzhou, Shenyang and Chongqing. Higher OC/EC ratio has been reported to be emitted  
761 from coal combustion (2.7) and biomass burning (6.6) than from motor vehicles (1.1) (Watson et  
762 al., 2001; Saarikoski et al., 2008). In the Northern China, the residential sector is the largest  
763 emitter of carbonaceous aerosols (Lei et al., 2011; Lu et al., 2011), which are formed by the  
764 inefficient combustion of fossil fuel and biomass in unregulated cooking and heating devices. For  
765 OC, the residential sector contribution can exceed 95% (Liu, et al., 2016c). Thus, the highest  
766 OC/EC ratio in Beijing indicates that residential emissions would also contributed considerably to  
767 the development of heavily polluted days.

768 Unlike in Beijing, the contributions of OM and EC were almost constant across the different  
769 pollution levels in Guangzhou, while the contribution of the secondary inorganic aerosols (SIA)  
770 increased slightly (Fig. 8b). Interestingly, the nitrate contribution increased faster than that of the  
771 sulfate when the pollution level increased from clean to heavily polluted, similar to the patterns of  
772 Beijing. Furthermore, the  $[\text{NO}_3^-]/[\text{SO}_4^{2-}]$  ratio increased continuously and it reported the highest  
773 ratio of  $[\text{NO}_3^-]/[\text{SO}_4^{2-}]$  (1.3) during the heavily polluted days in Guangzhou (Fig. 8). At the same  
774 time, the ratio of OC/EC was nearly constant with the aggravation of pollution, and it reported the  
775 lowest OC/EC ratio (1.6-1.8) among the four megacities. These results suggest the dominate  
776 contribution of local traffic emissions in the development of fine particulate pollution. The  
777 chemical evolution of  $\text{PM}_{2.5}$  at the background site of PRD was similar to that of the urban site at  
778 Guangzhou, although a significant contribution of SIA was observed when the pollution level  
779 increased from clean to moderately polluted (34% vs. 58%). Note that the contribution of sulfate  
780 increased sharply, suggesting that regional transports dominated the particle pollution during  
781 heavily polluted days.

782 Compared with Beijing, a reversed chemical evolution of  $\text{PM}_{2.5}$  for the different pollution  
783 levels was observed in Shenyang, with the OM fraction increasing sharply from 22% to 37%,  
784 while the SIA decreased slightly from 39% to 31% (Fig. 8c). Note that a steady increase of sulfate  
785 from slightly polluted days to heavily polluted days was observed. In addition, a nearly constant  
786 low ratio of  $[\text{NO}_3^-]/[\text{SO}_4^{2-}]$  (0.30-0.38) and continually increased ratio of OC/EC (2.3-4.5) was  
787 observed with the aggravation of pollution. These results suggest that enhanced local stationary  
788 emissions like coal combustion dominate the temporal evolution of  $\text{PM}_{2.5}$  on polluted days in  
789 Shenyang. The highest concentration of  $\text{Cl}^-$  in Shenyang than other cities in this study further  
790 support the significant contribution of coal combustion. A similar chemical evolution of  $\text{PM}_{2.5}$  was  
791 found at the background site of Changbai Mountain, which showed a significantly increased OM  
792 fraction and slightly decrease of SIA when the pollution level increased from clean to slighted  
793 polluted, indicating the enhanced contribution from local emissions like coal combustion for  
794 heating during slightly polluted days. Further support for this pattern is seen in the increase of the  
795 EC fraction (Fig. 8 g).

796 Similar to that in Guangzhou, the contribution of OM was almost constant for different  
797 pollution levels in Chongqing, while much higher contribution of SIA was observed, especially  
798 during the heavily polluted days. In addition, a steady increase of  $[\text{NO}_3^-]/[\text{SO}_4^{2-}]$  ratio was

799 observed, similar with those in Beijing and Guangzhou, suggesting the relatively more important  
800 contribution of mobile than stationary sources (Arimoto et al., 1996). Furthermore, the OC/EC  
801 ratio was also continually increased with the aggravation of pollution, and different from that in  
802 Guangzhou but similar with that in Shenyang. Note that the fraction of OM, sulfate and nitrate  
803 during the heavily polluted days in Chongqing was much higher than those in Beijing, Guangzhou  
804 and Shenyang, suggesting the higher oxidation capacity and therefore higher formation efficiency  
805 from gaseous pollutants (etc. SO<sub>2</sub>, NO<sub>x</sub>, VOCs) to secondary aerosol. These results suggest the  
806 importance of local traffic emissions and the formation of secondary aerosol in driving PM<sub>2.5</sub>  
807 pollution in Chongqing. The background site of Gongga Mountain shows decreased contributions  
808 of OM, EC, SIA and mineral dust when the pollution level increased from clean to slightly  
809 polluted days, similar to the pattern observed in Xinglong. Note that the unaccounted-for fraction  
810 was largely increased on slightly polluted days (33% vs. 10%), possibly due to the increase of  
811 aerosol-bound water related to the hygroscopic growth of aerosols at high RH values on slightly  
812 polluted days (Bian et al., 2014).

#### 813 4. Conclusions

814 We have established a national-level network (“Campaign on atmospheric Aerosol REsearch”  
815 network of China (CARE-China)) that conducted continuous monitoring of PM<sub>2.5</sub> mass  
816 concentrations at 40 ground observation station, including 20 urban sites, 12 background sites and  
817 8 rural/suburban sites. The average aerosol chemical composition was inferred from the filter  
818 samples from six paired urban and background sites, which represent the largest megacities and  
819 regional background areas in the five most polluted regions and the TAR of China. This study  
820 presents the first long-term dataset including three-year observations of online PM<sub>2.5</sub> mass  
821 concentrations (2012-2014) and one year observations of PM<sub>2.5</sub> compositions (2012-2013) from  
822 the CARE-China network. One of the major purposes of this study was to compare and contrast  
823 urban and background aerosol concentrations from nearby regions. The major findings include the  
824 following:

825 (1) The average PM<sub>2.5</sub> concentration from 20 urban sites is 73.2 μg/m<sup>3</sup> (16.8-126.9 μg/m<sup>3</sup>),  
826 which is three times greater than the average value of 12 background sites (11.2-46.5 μg/m<sup>3</sup>). The  
827 highest PM<sub>2.5</sub> concentrations were observed at the stations on the Guanzhong Plain (GZP) and the  
828 NCP. The PM<sub>2.5</sub> pollution is also a serious problem for the industrial regions of northeastern China  
829 and the Sichuan Basin and is a relatively less serious problem for the YRD and the PRD. The  
830 background PM<sub>2.5</sub> concentrations of the NCP, YRD and PRD were comparable to those of the  
831 nearby urban sites, especially for the PRD. A distinct seasonal variability of the PM<sub>2.5</sub> is observed,  
832 presenting peaks during the winter and minima during the summer at the urban sites, while the  
833 seasonal variations of PM<sub>2.5</sub> at the background sites vary in different part of China. Bimodal and  
834 unimodal diurnal variation patterns were identified at both the urban and background stations.

835 (2) The major PM<sub>2.5</sub> constituents across all the urban sites are OM (26.0%), SO<sub>4</sub><sup>2-</sup>(17.7%),  
836 mineral dust (11.8%), NO<sub>3</sub><sup>-</sup> (9.8%), NH<sub>4</sub><sup>+</sup> (6.6%), EC (6.0%), Cl<sup>-</sup> (1.2%) at 45% RH and  
837 unaccounted matter (20.7%). Similar chemical compositions of PM<sub>2.5</sub> were observed for the  
838 background sites and were associated with higher fractions of OM (33.2%) and lower fractions of  
839 NO<sub>3</sub><sup>-</sup> (8.6%) and EC (4.1%). Analysis of filter samples reveals that several PM<sub>2.5</sub> chemical  
840 components varied by more than an order of magnitude between sites. For urban sites, the OM

841 ranges from 12.6  $\mu\text{g}/\text{m}^3$  (Lhasa) to 23.3  $\mu\text{g}/\text{m}^3$  (Shenyang), the  $\text{SO}_4^{2-}$  ranges from 0.8  $\mu\text{g}/\text{m}^3$   
842 (Lhasa) to 19.7  $\mu\text{g}/\text{m}^3$  (Chongqing), the  $\text{NO}_3^-$  ranges from 0.5  $\mu\text{g}/\text{m}^3$  (Lhasa) to 11.9  $\mu\text{g}/\text{m}^3$   
843 (Shanghai) and the EC ranges from 1.4  $\mu\text{g}/\text{m}^3$  (Lhasa) to 7.1  $\mu\text{g}/\text{m}^3$  (Guangzhou). The  $\text{PM}_{2.5}$   
844 chemical species of the background sites exhibit larger spatial heterogeneities than those of the  
845 urban sites, suggesting the different contributions from regional anthropogenic and natural  
846 emissions and from the long-range transport to background areas.

847 (3) Notable seasonal variations of  $\text{PM}_{2.5}$  polluted days were observed, especially for the  
848 megacities in east-central China, resulting in frequent heavy pollution episodes occurring during  
849 the winter. The increasing contribution of secondary aerosol on polluted days was observed both  
850 for the urban and nearby background sites, suggesting fine particle pollution in the most polluted  
851 areas of China assumes a regional tendency, and the importance to address the emission reduction  
852 of secondary aerosol precursors. In addition, the chemical species dominating the evolutions of the  
853 heavily polluted events were different, while decreasing or constantly contribution of OM  
854 associated with increasing contribution of SIA characteristic evolution of  $\text{PM}_{2.5}$  in NCP, PRD and  
855 SWCR, the opposite phenomenon was observed in NECR. Further analysis from the  $[\text{NO}_3^-]/[\text{SO}_4^{2-}]$   
856 ratio and OC/EC ratio showed that fine particle pollution in Guangzhou and Shenyang was mainly  
857 attributed to the traffic emissions and coal combustion, respectively, while more complex and  
858 variable major sources including mobile vehicle emission and residential sources contributed to  
859 the development of heavily polluted days in Beijing. As for Chongqing, the higher oxidation  
860 capacity than other cities suggested it should pay more attention to the emission reduction of  
861 secondary aerosol precursors. These results suggest the different formation mechanisms of the  
862 heavy pollution in the most polluted city clusters, and unique mitigation measures should be  
863 developed for the different regions of China.

864 The seasonal and spatial patterns of urban and background aerosols emphasize the  
865 importance of understanding the variabilities of the concentrations of major aerosol species and  
866 their contributions to the  $\text{PM}_{2.5}$  budget. Comparisons of  $\text{PM}_{2.5}$  chemical compositions from urban  
867 and background sites of adjacent regions provided meaningful insights into aerosol sources and  
868 transport and into the role of urban influences on nearby rural regions. The integration of data  
869 from 40 sites from the CARE-China network provided an extensive spatial coverage of fine  
870 particle concentrations near the surface and could be used to validate model results and implement  
871 effective air pollution control strategies.

872

### 873 Acknowledgments

874 This study was supported by the Ministry of Science and Technology of China (Grant nos.  
875 2017YFC0210000), the National Natural Science Foundation of China (Grant nos. 41705110) and  
876 the Strategic Priority Research Program of the Chinese Academy of Sciences (Grant nos.  
877 XDB05020200 & XDA05100100). We acknowledge the tremendous efforts of all the scientists  
878 and technicians involved in the many aspects of the Campaign on atmospheric Aerosol REsearch  
879 network of China (CARE-China).

880

### 881 References

882 Arimoto, R., Duce, R. A., Savoie, D. L., Prospero, J., Talbot, R., Cullen, J., Tomza, U., Lewis, N., and Ray, B.:

883 Relationships among aerosol constituents from Asia and the North Pacific during PEM-West A, *J. Geophys. Res.*,  
884 101, 2011-2023, 1996.

885 Bell, M. L., Dominici, F., Ebisu, K., Zeger, S. L., and Samet, J. M.: Spatial and temporal variation in PM<sub>2.5</sub>  
886 chemical composition in the United States for health effects studies. *Environ Health Perspect.*, 115, 989-995, 2007.

887 Bian, Y. X., Zhao, C. S., Ma, N., Chen, J., and Xu, W. Y.: A study of aerosol liquid water content based on  
888 hygroscopicity measurements at high relative humidity in the North China Plain. *Atmos. Chem. Phys.*, 14,  
889 6417-6426, 2014.

890 Boyouk, N., Léon, J. F., Delbarre, H., Podvin, T., and Deroo, C.: Impact of the mixing boundary layer on the  
891 relationship between PM<sub>2.5</sub> and aerosol optical thickness. *Atmos. Environ.*, 44(2), 271-277, 2010.

892 Chan, C. K., and Yao X. H.: Air pollution in mega cities in China. *Atmos. Environ.*, 42(1), 1-42, 2008.

893 Chen, W. H., Wang, X. M., Zhou, S. Z., Cohen, J. B., Zhang, J., Wang, Y., Chang, M., Zeng, Y., Liu, Y., Ling, Z.,  
894 Liang, G., and Qiu, X.: Chemical Composition of PM<sub>2.5</sub> and its Impact on Visibility in Guangzhou, Southern China.  
895 *Aerosol Air Qual. Res.*, 16, 2349-2361, 2016.

896 Chen, Y., Xie, S. D., Luo, B., and Zhai, C. Z.: Particulate pollution in urban Chongqing of southwest China:  
897 Historical trends of variation, chemical characteristics and source apportionment. *Sci. Total Environ.*, 584-585,  
898 523-534, 2017.

899 Chen, Z., Wang, J. N., Ma, G. X., and Zhang, Y. S.: China tackles the health effects of air pollution. *Lancet*, 382,  
900 1959-1960, 2013.

901 Cheng, Z., Wang, S., Fu, X., Watson, J. G., Jiang, J., Fu, Q., Chen, C., Xu, B., Yu, J., Chow, J. C., and Hao, J.:  
902 Impact of biomass burning on haze pollution in the Yangtze River delta, China: a case study in summer 2011.  
903 *Atmos. Chem. Phys.*, 14 (9), 4573-4585, 2014.

904 Cheng, Z., Luo, L., Wang, S., Wang, Y., Sharma, S., Shimadera, H., Wang, X., Bressi, M., Maura de Miranda, R.,  
905 Jiang, J., Zhou, W., Fajardo, O., Yan, N., Hao, J.: Status and characteristics of ambient PM<sub>2.5</sub> pollution in global  
906 megacities. *Environ. Int.*, 89-90, 212-221, 2016.

907 Cong, Z., Kang, S., Luo, C., Li, Q., Huang, J., Gao, S. P., and Li, X. D.: Trace elements and lead isotopic  
908 composition of PM<sub>10</sub> in Lhasa, Tibet. *Atmos. Environ.*, 45, 6210-6215, 2011.

909 Cusack, M., Alastuey, A., P´erez, N., Pey, J., and Querol, X.: Trends of particulate matter (PM<sub>2.5</sub>) and chemical  
910 composition at a regional background site in the Western Mediterranean over the last nine years (2002–2010).  
911 *Atmos. Chem. Phys.*, 12, 8341-8357, 2012.

912 Dickerson, R.R., Li, C., Li, Z., Marufu, L.T., Stehr, J.W., McClure, B., Krotkov, N., Chen, H., Wang, P., Xia, X.,  
913 Ban, X., Gong, F., Yuan, J., and Yang, J.: Aircraft observations of dust and pollutants over northeast China: insight  
914 into the meteorological mechanisms of transport. *J. Geophys. Res.*, 112, D24S90, doi: 10.1029/2007JD008999,  
915 2007.

916 Eeftens, M., Tsai, M.-Y., Ampe, C., Anwander, B., Beelen, R., Bellander, T., Cesaroni, G., Cirach, M., Cyrys, J.,  
917 Hoogh, K. D., Nazelle, A. D., Vocht, F. D., Declercq, C., Dedele, A., Eriksen, K., Galassi, C., Grazuleviciene, R.,  
918 Grivas, G., Heinrich, J., Hoffmann, B., Iakovides, M., Ineichen, A., Katsouyanni, K., Korek, M., Krämer, U.,  
919 Kuhlbusch, T., Lanki, T., Madsen, C., Meliefste, K., Mölter, A., Mosler, G., Nieuwenhuijsen, M., Oldenwening,  
920 M., Pennanen, A., Probst-Hensch, N., Quass, U., Raaschou-Nielsen, O., Ranzi, A., Stephanou, E., Sugiri, D.,  
921 Udvardy, O., Vaskövi, É., Weinmayr, G., Brunekreef, B., and Hoek, G.: Spatial variation of PM<sub>2.5</sub>, PM<sub>10</sub>, PM<sub>2.5</sub>  
922 absorbance and PM coarse concentrations between and within 20 European study areas and the relationship with  
923 NO<sub>2</sub> - Results of the ESCAPE project. *Atmos. Environ.*, 62, 303-317, 2012.

924 Fu, X., Wang, S. X., Zhao, B., Xing, J., Cheng, Z., Liu, H., and Hao, J. M.: Emission inventory of primary

925 pollutants and chemical speciation in 2010 for the Yangtze River Delta region, China. *Atmos. Environ.*, 70, 39-50,  
926 2013.

927 Fu, X., Wang, S. X., Cheng, Z., Xing, J., Zhao, B., Wang, J. D., and Hao, J. M.: Source, transport and impacts of a  
928 heavy dust event in the Yangtze River Delta, China, in 2011. *Atmos. Chem. Phys.*, 14 (3), 1239-1254, 2014.

929 Gehrig, R., and Buchmann, B.: Characterising seasonal variations and spatial distribution of ambient PM<sub>10</sub> and  
930 PM<sub>2.5</sub> concentrations based on long-term Swiss monitoring data. *Atmos. Environ.*, 37, 2571-2580, 2003.

931 Guo, S., Hu, M., Zamora, M. L., Peng, J., Shang, D., Zheng, J., Du, Z., Wu, Z., Shao, M., Zeng, L., Molina, M. J.,  
932 and Zhang, R.: Elucidating severe urban haze formation in China. *Proc. Nat. Acad. Sci. U.S.A.* 111, 17373-17378,  
933 2014.

934 Hand, J. L., Schichtel, B. A., Pitchford, M., Malm, W. C., and Frank, N. H.: Seasonal composition of remote and  
935 urban fine particulate matter in the United States. *J. Geophys. Res.*, 117, D05209, doi: 10.1029/2011JD017122,  
936 2012.

937 He, K. B., Yang, F. M., Ma, Y. L., Zhang, Q., Yao, X. H., Chan, C. K., Cadle, S., Chan, T., and Mulawa, P.: The  
938 characteristics of PM<sub>2.5</sub> in Beijing, China. *Atmos. Environ.*, 35(29), 4959-4970, 2001.

939 Hoffer, A., Gelencser, A., Guyon, P., Kiss, G., Schmid, O., Frank, G. P., Artaxo, P. and Andreae, M. O.: Optical  
940 properties of humic-like substances (HULIS) in biomass-burning aerosols. *Atmos. Chem. Phys.*, 6, 3563-3570,  
941 2006.

942 Huang, R. J., Zhang, Y., Bozzetti, C., Ho, K., Cao, J., Han, Y., Daellenbach, K., Slowik, J., Platt, S., Canonaco, F.,  
943 Zotter, P., Wolf, R., Pieber, S., Bruns, E., Crippa, M., Ciarelli, G., Piazzalunga, A., Schwikowski, M., Abbaszade,  
944 G., Schnelle-Kreis, J., Zimmermann, R., An, Z., Szidat, S., Baltensperger, U., Haddad, I., and Prévôt, A.: High  
945 secondary aerosol contribution to particulate pollution during haze events in China. *Nature*, 514, 218-222, 2014.

946 Huang, Y., Li, L., Li, J., Wang, X., Chen, H., Chen, J., Yang, X., Gross, D. S., Wang, H., Qiao, L., and Chen, C.: A  
947 case study of the highly time-resolved evolution of aerosol chemical and optical properties in urban Shanghai,  
948 China. *Atmos. Chem. Phys.*, 13(8), 3931-3944, 2013.

949 IPCC: *Climate Change 2013: The Physical Science Basis: Summary for Policymakers*, Cambridge, UK, 2013.

950 Janssen, N. A. H., Fischer, P., Marra, M., Ameling, C., and Cassee, F. R.: Short-term effects of PM<sub>2.5</sub>, PM<sub>10</sub> and  
951 PM<sub>2.5-10</sub> on daily mortality in the Netherlands. *Sci. Total. Environ.*, 463-464, 20-26, 2013.

952 **Lei, Y., Zhang, Q., He, K. B., Streets, D. G.: Primary anthropogenic aerosol emission trends for China, 1990-2005.**  
953 ***Atmos. Chem. Phys.*, 11(3), 931-954, 2011.**

954 Li, L., Chen, C. H., Fu, J. S., Huang, C., Streets, D. G., Huang, H. Y., Zhang, G. F., Wang, Y. J., Jang, C. J., Wang,  
955 H. L., Chen, Y. R., and Fu, J. M.: Air quality and emissions in the Yangtze River Delta, China. *Atmos. Chem. Phys.*,  
956 11, 1621-1639, 2011

957 Li, Y. C., Yu, J. Z., Ho, S. S. H., Yuan, Z. B., Lau, A. K. H., and Huang X. F.: Chemical characteristics of PM<sub>2.5</sub> and  
958 organic aerosol source analysis during cold front episodes in Hong Kong, China. *Atmos. Res.*, 118, 41-51, 2012.

959 Liu, Z. R., Hu, B., Wang, L. L., Wu, F. K., Gao, W. K., and Wang, Y. S.: Seasonal and diurnal variation in  
960 particulate matter (PM<sub>10</sub> and PM<sub>2.5</sub>) at an urban site of Beijing: analyses from a 9-year study. *Environ. Sci. Pollut.*  
961 *Res.*, 22, 627-642, 2015.

962 Liu, L., Zhang, X., Wang, S., Zhang, W., and Lu, X.: Bulk sulfur (S) deposition in China. *Atmos. Environ.*, 135,  
963 41-49, 2016b.

964 **Liu, J., Mauzerall, D. L., Chen, Q., Zhang, Q., Song, Y., Peng, W., Klimont, Z., Qiu, X., Zhang, S., Hu, M., Lin, W.,**  
965 **Smith, K. R., and Zhu, Tong.: Air pollutant emissions from Chinese households: A major and underappreciated**  
966 **ambient pollution source. *PANS*, 113(28), 7756-7761, 2016c.**

967 Liu, Z. R., Wang, Y. S., Hu, B., Ji, D. S., Zhang, J. K., Wu, F. K., Wan, X. and Wang, Y. H.: Source appointment of  
968 fine particle number and volume concentration during severe haze pollution in Beijing in January 2013. *Environ.*  
969 *Sci. Pollut. Res.*, 23(7), 6845-6860, 2016a.

970 Liu, Z. R., Wang, Y. S., Liu, Q., Liu, L. N., and Zhang, D. Q.: Pollution Characteristics and Source of the  
971 Atmospheric Fine Particles and Secondary Inorganic Compounds at Mount Dinghu in Autumn Season (in Chinese).  
972 *Environ. Sci.*, 32, 3160-3166, 2011.

973 Liu, Z. R., Xie, Y., Hu, B., Wen, T., Xin, J., Li, X., Wang, Y. S.: Size-resolved aerosol water-soluble ions during the  
974 summer and winter seasons in Beijing: Formation mechanisms of secondary inorganic aerosols. *Chemosphere*, 183,  
975 119-131, 2017.

976 Lu, Z., Streets, D. G., Zhang, Q., Wang, S., Carmichael, G. R., Cheng, Y. F., Wei, C., Chin, M., Dieh, T., and Tan,  
977 Q.: Sulfur dioxide emissions in China and sulfur trends in East Asia since 2000. *Atmos. Chem. Phys.*, 10,  
978 6311-6331, 2010.

979 Lu, Z., Zhang, Q., Streets, D. G.: Sulfur dioxide and primary carbonaceous aerosol emissions in China and India,  
980 1996-2010. *Atmos. Chem. Phys.*, 11(18), 9839-9864, 2011.

981 Malm, W. C., Schichtel, B. A., Pitchford, M. L., Ashbaugh, L. L., and Eldred, R. A.: Spatial and monthly trends in  
982 speciated fine particle concentration in the United States. *J. Geophys. Res.*, 109, D03306, doi:  
983 10.1029/2003JD003739, 2004.

984 Mamtimin, B., and Meixner, F. X.: Air pollution and meteorological processes in the growing dryland city of  
985 Urumqi (Xinjiang, China). *Sci. Total Environ.*, 409(7), 1277-1290, 2011.

986 Mao, Y. H., Liao, H., and Chen, H. S.: Impacts of East Asian summer and winter monsoons on interannual  
987 variations of mass concentrations and direct radiative forcing of black carbon over eastern China. *Atmos. Chem.*  
988 *Phys.*, 17, 4799-4816, 2017.

989 Mason, B.: *Principles of Geochemistry*, New York, Wiley, 1966.

990 Mauderly, J. L., and Chow, J. C.: Health effects of organic aerosols. *Inhal. Toxicol.*, 20, 257-288, 2008.

991 Niu, Z. C., Zhang, F. W., Chen, J. S., Yin, L. Q., Wang, S., and Xu, L. L.: Carbonaceous species in PM<sub>2.5</sub> in the  
992 coastal urban agglomeration in the Western Taiwan Strait Region, China. *Atmos. Res.*, 122, 102-110, 2013.

993 Oanh, N. T. K., Upadhyay, N., Zhuang, Y. H., Hao, Z. P., Murthy, D. V. S., Lestari, P., Villarin, J. T., Chengchua, K.,  
994 Co, H. X., Dung, N. T., and Lindgren, E. S.: Particulate air pollution in six Asian cities: Spatial and temporal  
995 distributions, and associated sources. *Atmos. Environ.*, 40, 3367-3380, 2006.

996 Pan, Y. P., Wang, Y. S., Sun, Y., Tian, S. L., and Cheng, M. T.: Size-resolved aerosol trace elements at a rural  
997 mountainous site in Northern China: Importance of regional transport. *Sci. Total Environ.*, 461, 761-771, 2013.

998 Patashnick, H., and Rupprecht, E.: Continuous PM<sub>10</sub> measurements using the tapered element oscillating  
999 microbalance. *J. Air Waste Manage.*, 41, 1079-1083, 1991.

1000 Putaud, J. P., Van Dingenen, R., Alastuey, A., Bauer, H., Birmili, W., Cyrys, J., Flentje, H., Fuzzi, S., Gehrig, R.,  
1001 Hansson, H. C., Harrison, R. M., Herrmann, H., Hitzenberger, R., Hüglin, C., Jones, A. M., Kasper-Giebl, A., Kiss,  
1002 G., Kousa, A., Kuhlbusch, T. A. J., Löschau, G., Maenhaut, W., Molnar, A., Moreno, T., Pekkanen, J., Perrino, C.,  
1003 Pitz, M., Puxbaum, H., Querol, X., Rodriguez, S., Salma, I., Schwarz, J., Smolik, J., Schneider, J., Spindler, G., ten  
1004 Brink, H., Tursic, J., Viana, M., Wiedensohler, A., and Raes, F.: A European aerosol phenomenology - 3: Physical  
1005 and chemical characteristics of particulate matter from 60 rural, urban, and kerbside sites across Europe. *Atmos.*  
1006 *Environ.*, 44, 1308-1320, 2010.

1007 Quan, J. N., Tie, X. X., Zhang, Q., Liu, Q., Li, X., Gao, Y., and Zhao, D. L.: Characteristics of heavy aerosol  
1008 pollution during the 2012-2013 winter in Beijing, China. *Atmos. Environ.*, 88, 83-89, 2014.

1009 Saarikoski, S., Timonen, H., Saarnio, K., Aurela, M., Järvi, L., Keronen, P., Kerminen, V.-M., and Hillamo, R.:  
1010 Sources of organic carbon in fine particulate matter in northern European urban air, *Atmos. Chem. Phys.*, 8,  
1011 6281-6295, <https://doi.org/10.5194/acp-8-6281-2008>, 2008.

1012 Seinfeld, J. H., and Pandis, S. N.: *Atmospheric Chemistry and Physics: from Air Pollution to Climate Change*.  
1013 Wiley, New York, USA, 2016.

1014 Sun, Q. H., Hong, X. R., and Wold, L. E.: Cardiovascular Effects of Ambient Particulate Air Pollution Exposure.  
1015 *Circulation*, 121(25), 2755-2765, 2010.

1016 Tao, J., Zhang, L. M., Ho, K. F., Zhang, R. J., Lin, Z. J., Zhang, Z. S., Lin, M., Cao, J. J., Liu, S. X., and Wang, G.  
1017 H.: Impact of PM<sub>2.5</sub> chemical compositions on aerosol light scattering in Guangzhou - the largest megacity in  
1018 South China. *Atmos. Res.*, 135, 48-58, 2014.

1019 Tao, J., Zhang, L. M., Cao, J. J., Zhong, L. J., Chen, D. S., Yang, Y. H., Chen, D. H., Chen, L. G., Zhang, Z. S., Wu,  
1020 Y. F., Xia, Y. J., Ye, S. Q., and Zhang, R. J.: Source apportionment of PM<sub>2.5</sub> at urban and suburban areas of the  
1021 Pearl River Delta region, south China - With emphasis on ship emissions. *Sci. Total Environ.*, 574, 1559-1570,  
1022 2017.

1023 Turpin, B. J., and Lim, H. J.: Species contributions to PM<sub>2.5</sub> mass concentrations: Revisiting common assumptions  
1024 for estimating organic mass. *Aerosol Sci. Technol.*, 35, 602-610, 2001.

1025 Verma, R. L., Sahu, L. K., Kondo, Y., Takegawa, N., Han, S., Jung, J. S., Kim, Y. J., Fan, S., Sugimoto, N., Shammaa,  
1026 M. H., Zhang, Y. H., and Zhao, Y.: Temporal variations of black carbon in Guangzhou, China, in summer 2006.  
1027 *Atmos. Chem. Phys.*, 10, 6471-6485, 2010.

1028 Viana, M., X., Querol, A., Alastuey, F., Ballester, S., Llop, A., Esplugues, R., Fernandez-Patier, S., dos Santos, G.,  
1029 and Herce, M. D.: Characterising exposure to PM aerosols for an epidemiological study. *Atmos. Environ.*, 42(7),  
1030 1552-1568, 2008.

1031 Wan, X., Kang, S. C., Xin, J. Y., Liu, B., Wen, T. X., Wang, P. L., Wang, Y. S., and Cong, Z. Y.: Chemical  
1032 composition of size-segregated aerosols in Lhasa city, Tibetan Plateau. *Atmos. Res.*, 174-175, 142-150, 2016.

1033 Wang, Y. S., Yao, L., Wang, L. L., Liu, Z. R., Ji, D. S., Tang, G. Q., Zhang, J. K., Sun, Y., Hu, B., and Xin, J. Y.:  
1034 Mechanism for the formation of the January 2013 heavy haze pollution episode over central and eastern China. *Sci.*  
1035 *China: Earth Sci.*, 57, 14-25, 2014.

1036 Wang, G. H., Zhou, B. H., Cheng, C. L., Cao, J. J., Li, J. J., Meng, J. J., Tao, J., Zhang, R. J., and Fu, P. Q.: Impact  
1037 of Gobi desert dust on aerosol chemistry of Xi'an, inland China during spring 2009: differences in composition and  
1038 size distribution between the urban ground surface and the mountain atmosphere. *Atmos. Chem. Phys.*, 13(2),  
1039 819-835, 2013.

1040 Wang, H. B., Tian, M., Li, X., Chang, Q., Cao, J., Yang, F., Ma, Y., He, K.: Chemical Composition and Light  
1041 Extinction Contribution of PM<sub>2.5</sub> in Urban Beijing for a 1-Year Period. *Aerosol and Air Quality Research*, 15,  
1042 2200-2211, 2015a.

1043 Wang, H. L., Qiao, L. P., Lou, S. R., Zhou, M., Ding, A. J., Huang, H. Y., Chen, J. M., Wang, Q., Tao, S. K., Chen,  
1044 C. H., Li, L., and Huang, C.: Chemical composition of PM<sub>2.5</sub> and meteorological impact among three years in  
1045 urban Shanghai, China. *J. Clean. Prod.*, 112, 1302-1311, 2016.

1046 Wang, Y. Q., Zhang, X. Y., Sun, J. Y., Zhang, X. C., Che, H. Z., and Li, Y.: Spatial and temporal variations of the  
1047 concentrations of PM<sub>10</sub>, PM<sub>2.5</sub> and PM<sub>1</sub> in China. *Atmos. Chem. Phys.*, 15, 13585-13598, 2015b.

1048 Watson, J. G., Chow, J. C., and Houck, J. E.: PM<sub>2.5</sub> chemical source profiles for vehicle exhaust, vegetative burning,  
1049 geological material, and coal burning in Northwestern Colorado during 1995, *Chemosphere*, 43, 1141-1151,  
1050 [https://doi.org/10.1016/S0045-6535\(00\)00171-5](https://doi.org/10.1016/S0045-6535(00)00171-5), 2001.

1051 [Westerdahl, D., Wang, X., Pan, X. C. and Zhang, K. M.: Characterization of on-road vehicle emission factors and](#)  
1052 [microenvironmental air quality in Beijing, China. \*Atmos. Environ.\* 43, 697-705, 2009.](#)

1053 Wu, F. K., Yu, Y., Sun, J., Zhang, J. K., Wang, J., Tang, G. Q., and Wang, Y. S.: Characteristics, source  
1054 apportionment and reactivity of ambient volatile organic compounds at Dinghu Mountain in Guangdong Province,  
1055 China. *Sci. Total Environ.*, 548-549, 347-359, 2016.

1056 Xia, X. A., Chen, H. B., Wang, P. C., Zhang, W. X., Goloub, P., Chatenet, B., Eck, T. F., and Holben, B. N.:  
1057 Variation of column-integrated aerosol properties in a Chinese urban region. *J. Geophys. Res.-Atmos.*, 111,  
1058 D05204, doi: 10.1029/2005JD006203, 2006.

1059 Xin, J., Wang, Y., Pan, Y., Ji, D., Liu, Z., Wen, T., Wang, Y., Li, X., Sun, Y., Sun, J., Wang, P., Wang, G., Wang, M.,  
1060 Cong, Z., Song, T., Hu, B., Wang, L., Tang, G., Gao, W., Guo, Y., Miao, H., Tian, S., and Wang, L.: The Campaign  
1061 on atmospheric Aerosol REsearch network of China: CARE-China. *BAMS*, 96(7), 1137-1155, 2015.

1062 Xing, L., Fu, T. M., Cao, J. J., Lee, S. C., Wang, G. H., Ho, K. F., Cheng, M. C., You, C. F., and Wang, T. J.:  
1063 Seasonal and spatial variability of the OM/OC mass ratios and high regional correlation between oxalic acid and  
1064 zinc in Chinese urban organic aerosols. *Atmos. Chem. Phys.*, 13, 4307-4318, 2013.

1065 Xu, J. S., Xu, M. X., Snape, C., He, J., Behera, S. N., Xu, H. H., Ji, D. S., Wang, C. J., Yu, H., Xiao, H., Jiang, Y. J.,  
1066 Qi, B., and Du, R. G.: Temporal and spatial variation in major ion chemistry and source identification of secondary  
1067 inorganic aerosols in Northern Zhejiang Province, China. *Chemosphere*, 179, 316-330, 2017.

1068 Yang, F., Tan, J., Zhao, Q., Du, Z., He, K., Ma, Y., Duan, F., and Chen, G.: Characteristics of PM<sub>2.5</sub> speciation in  
1069 representative megacities and across China. *Atmos. Chem. Phys.*, 11(11), 5207-5219, 2011.

1070 [Yang Y. J., Wang Y. S, Wen T. X, Li, W., Zhao, Y., Li L.: Elemental composition of PM<sub>2.5</sub> and PM<sub>10</sub> at Mount](#)  
1071 [Gongga in China during 2006. \*Atmos. Res.\* 93, 801-810, 2009.](#)

1072 Ye, B., Ji, X., Yang, H., Yao, X., Chan, C. K., Cadle, S. H., Chan, T., and Mulawa, P. A.: Concentration and  
1073 chemical composition of PM<sub>2.5</sub> in Shanghai for a 1-year period. *Atmos. Environ.*, 37, 499-510, 2003.

1074 Zhang, C., Zhou, R., and Yang, S.: Implementation of clean coal technology for energy-saving and emission  
1075 reduction in Chongqing. *Environment and Ecology in the Three Gorges (in Chinese)*, 3, 52-56, 2010.

1076 Zhang, J. K., Sun, Y., Wu, F. K., Sun, J., and Wang, Y. S.: The characteristics, seasonal variation and source  
1077 apportionment of VOCs at Gongga Mountain, China. *Atmos. Environ.*, 88, 297-305, 2014c.

1078 Zhang, L. W., Chen, X., Xue, X. D., Sun, M., Han, B., Li, C. P., Ma, J., Yu, H., Sun, Z. R., Zhao, L. J., Zhao, B. X.,  
1079 Liu, Y. M., Chen, J., Wang, P. P., Bai, Z. P., and Tang, N. J.: Long-term exposure to high particulate matter  
1080 pollution and cardiovascular mortality: A 12-year cohort study in four cities in northern China. *Environ. Int.*, 62,  
1081 41-47, 2014a.

1082 Zhang, N. N., Cao, J. J., Liu, S. X., Zhao, Z. Z., Xu, H. M., and Xiao, S.: Chemical composition and sources of  
1083 PM<sub>2.5</sub> and TSP collected at Qinghai Lake during summertime. *Atmos. Res.*, 138, 213-222, 2014b.

1084 Zhang, X. Y., Wang, Y. Q., Niu, T., Zhang, X. C., Gong, S. L., Zhang, Y. M., and Sun, J. Y.: Atmospheric aerosol  
1085 compositions in China: spatial/temporal variability, chemical signature, regional haze distribution and comparisons  
1086 with global aerosols. *Atmos. Chem. Phys.* 12 (2), 779-799, 2012.

1087 Zhang, Y. L., and Cao, F.: Fine particulate matter (PM<sub>2.5</sub>) in China at a city level. *Sci. Rep.*, 5: 14884. 2015.

1088 Zhao, M. F., Huang, Z. S., Qiao, T., Zhang, Y. K., Xiu, G. L., and Yu, J. Z.: Chemical characterization, the transport  
1089 pathways and potential sources of PM<sub>2.5</sub> in Shanghai: seasonal variations. *Atmos. Res.*, 158, 66-78, 2015.

1090 Zhao, P. S., Dong, F., Yang, Y. D., He, D., Zhao, X. J., Zhang, W. Z., Yao, Q., and Liu, H. Y.: Characteristics of  
1091 carbonaceous aerosol in the region of Beijing, Tianjin, and Hebei, China. *Atmos. Environ.*, 71, 389-398, 2013a.

1092 Zhao, X. J., Zhao, P. S., Xu, J., Meng, W., Pu, W. W., Dong, F., He, D., and Shi, Q. F.: Analysis of a winter regional

1093 haze event and its formation mechanism in the North China Plain. *Atmos. Chem. Phys.*, 13(11), 5685-5696, 2013b.  
1094 Zheng, J., Zhang, L., Che, W., Zheng, Z., and Yin, S.: A highly resolved temporal and spatial air pollutant emission  
1095 inventory for the Pearl River Delta region, China and its uncertainty assessment. *Atmos. Environ.* 43, 5112-5122,  
1096 2009.  
1097 Zhou, S. Z., Wang, Z., Gao, R., Xue, L., Yuan, C., Wang, T., Gao, X., Wang, X., Nie, W., Xu, Z., Zhang, Q., and  
1098 Wang, W.: Formation of secondary organic carbon and long-range transport of carbonaceous aerosols at Mount  
1099 Heng in South China. *Atmos. Environ.*, 63, 203-212, 2012.  
1100 [Zhu, K., Zhang, J., Liou, P. J.: Evaluation and Comparison of Continuous Fine Particulate Matter Monitors for](#)  
1101 [Measurement of Ambient Aerosols, \*J. Air & Waste Manage. Assoc.\*, 57:12, 1499-1506, 2007.](#)  
1102 Zimmermann, R.: Aerosols and health: a challenge for chemical and biological analysis. *Anal Bioanal Chem.*, 407,  
1103 5863-5867, 2015.  
1104 Zou, X. K., and Zhai, P. M.: Relationship between vegetation coverage and spring dust storms over northern China.  
1105 *J. Geophys. Res.*, 109, D03104, doi: 10.1029/2003JD003913, 2004.  
1106

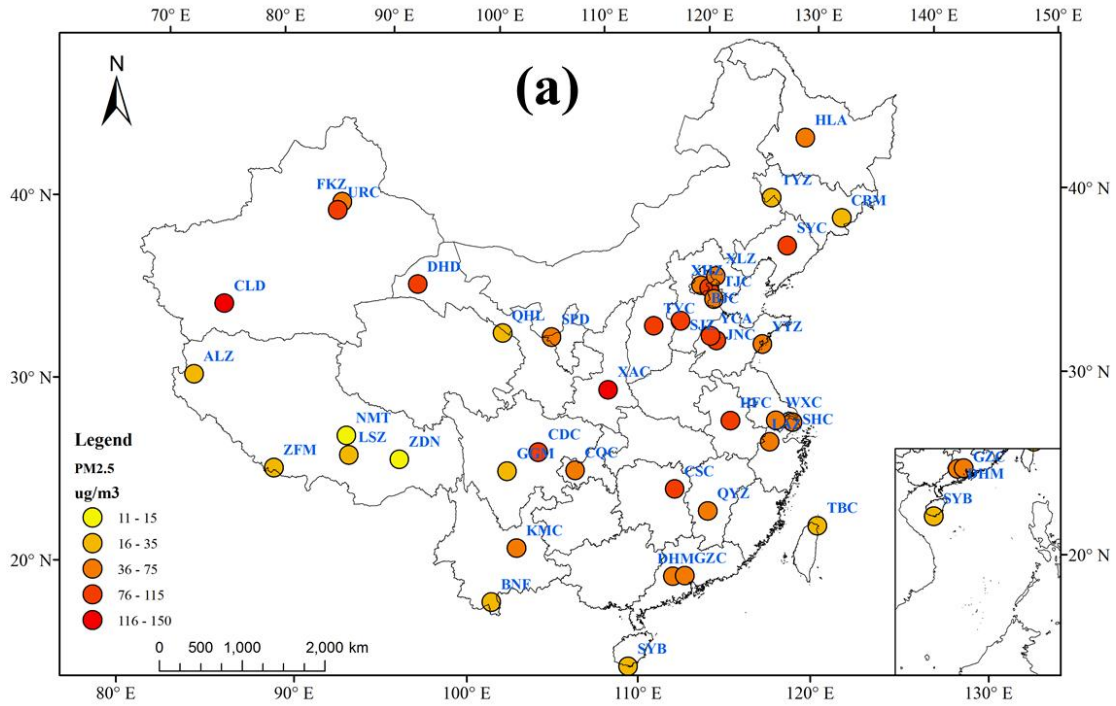
Table 1 Geographic information and three-year mean PM<sub>2.5</sub> concentration of the monitor stations.

Station/Code	Latitude, Longitude	Altitude(m)	Station type	Mean( $\mu\text{g}/\text{m}^3$ )	N(day)
Beijing/BJC	39.97°N, 116.37°E	45	Northern city	69.4±54.8	1077
Cele/CLD	37.00°N, 80.72°E	1306	Northwestern country	126.9±155.4	600
Changbai Mountain/CBM	42.40°N, 128.01°E	738	Northeastern background	17.6±12.6	807
Changsha/CSC	28.21°N, 113.06°E	45	Central city	77.9±45.4	1045
Chengdu/CDC	30.67°N, 104.06°E	506	Southwestern city	102.2±66.2	1008
Chongqing/CQC	29.59°N, 106.54°E	259	Southwestern city	65.1±35.8	972
Dinghu Mountain/DHM	23.17°N, 112.50°E	90	Pearl River Delta background	40.1±25.0	954
Dunhuang/DHD	40.13°N, 94.71°E	1139	Desert town	86.2±94.3	726
Fukang/FKZ	44.28°N, 87.92°E	460	Northwestern country	69.9±69.6	960
Gongga Mountain/GGM	29.51°N, 101.98°E	1640	Southwestern background	25.5±15.5	869
Guangzhou/GZC	23.16°N, 113.23°E	43	Southern city	44.1±23.8	772
Hailun/HLA	47.43°N, 126.63°E	236	Northeastern country	41.6±45.0	1076
Hefei/HFC	31.86°N, 117.27°E	24	Eastern city	80.4±45.3	909
Ji'nan/JNC	36.65°N, 117.00°E	70	Northern city	107.8±57.4	701
Kunming/KMC	25.04°N, 102.73°E	1895	Southwestern city	47.0±25.2	967
Lhasa/LSZ	29.67°N, 91.33°E	3700	Tibet city	30.6±21.3	600
Lin'an/LAZ	30.30°N, 119.73°E	139	Eastern background	46.5±27.2	1086
Mount Everest/ZFM	28.21°N, 86.56°E	4700	Tibet background	24.4±25.1	390
Namtso/NMT	30.77°N, 90.98°E	4700	Tibet background	11.2±6.9	499
Nagri/ALZ	32.52°N, 79.89°E	4300	Tibet background	19.5±12.4	72
Qianyanzhou/QYZ	26.75°N, 115.07°E	76	Southeastern country	52.1±28.4	927
Qinghai Lake/QHL	37.62°N, 101.32°E	3280	Tibet background	16.2±17.0	590
Sanya/SYB	18.22°N, 109.47°E	8	Southern island city	16.8±13.1	595
Shanghai/SHC	31.22°N, 121.48°E	9	Eastern city	56.2±59.4	822
Shapotou/SPD	37.45°N, 104.95°E	1350	Desert background	51.1±33.3	1016
Shenyang/SYC	41.50°N, 123.40°E	49	Northeastern city	77.6±41.2	926
Shijiazhuang/SJZ	38.03°N, 114.53°E	70	Northern city	105.1±92.7	1031
Taipei/TBC	25.03°N, 121.90°E	150	Island city	22.1±10.7	1083
Taiyuan/TYC	37.87°N, 112.53°E	784	Northern city	111.5±74.9	987
Tianjin/TJC	39.08°N, 117.21°E	9	Northern city	69.9±49.6	1034
Tongyu/TYZ	44.42°N, 122.87°E	160	Inner Mongolia background	24.5±24.5	757
Urumchi/URC	43.77°N, 87.68°E	918	Northwestern city	104.1±145.2	776
Wuxi/WXC	31.50°N, 120.35°E	5	Eastern city	65.2±36.8	1003
Xi'An/XAC	34.27°N, 108.95°E	397	Central city	125.8±108.2	1077
Xianghe/XHZ	39.76°N, 116.95°E	25	North China suburbs	83.7±62.3	1084
Xinglong/XLZ	40.40°N, 117.58°E	900	North China background	39.8±34.0	1035
Xishuangbanna/BNF	21.90°N, 101.27°E	560	Southwestern rain forest	25.0±18.7	707
Yantai/YTZ	36.05°N, 120.27°E	47	East China sea coast city	51.1±36.7	915
Yucheng/YCA	36.95°N, 116.60°E	22	North China country	102.8±61.8	1008
Zangdongnan/ZDN	29.77°N, 94.73°E	2800	Southern Tibet forest	12.3±8.0	475

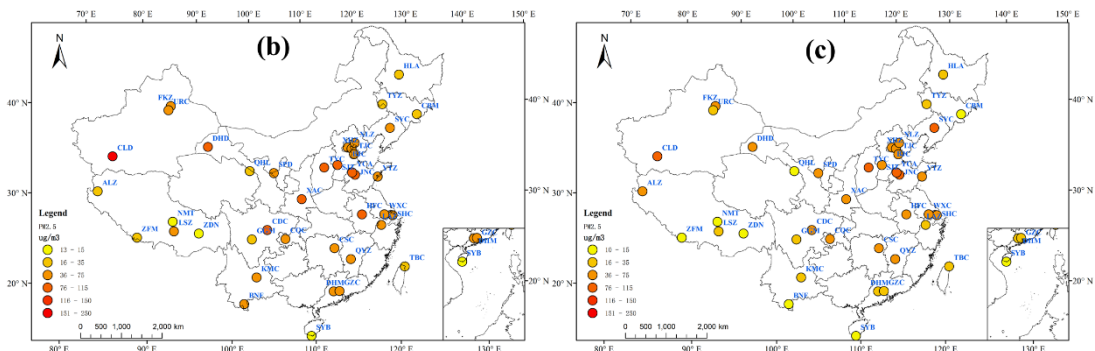
1108 Table 2 Summary of the concentrations of PM<sub>2.5</sub> and its components (µg/m<sup>3</sup>) in urban and  
 1109 background sites.

Station	PM <sub>2.5</sub>	OM	EC	NO <sub>3</sub> <sup>-</sup>	SO <sub>4</sub> <sup>2-</sup>	NH <sub>4</sub> <sup>+</sup>	MD*	Cl <sup>-</sup>	Unaccounted**
Urban sites									
BJC(n=88)	71.7(36.0)	19.1(11.0)	4.1(1.1)	9.3(7.5)	11.9(8.2)	5.3(2.7)	4.7(2.9)	0.7(1.0)	16.5(11.8)
SHC(n=120)	68.4(20.3)	17.1(4.5)	2.0(0.6)	11.9(5.0)	13.6(6.4)	5.8(2.1)			18.1(4.9)
GZC(n=106)	75.3(37.7)	16.7(10.0)	7.1(4.8)	7.2(7.9)	13.1(7.9)	4.8(3.5)	7.3(3.3)	1.0(1.1)	18.1(13.1)
LSZ(n=60)	36.4(18.7)	12.6(1.9)	1.4(0.6)	0.5(0.2)	0.8(0.4)	0.4(0.2)	11.6(12.9)	0.3(0.1)	8.8(7.8)
SYC(n=36)	81.8(55.6)	23.3(22.3)	5.2(3.4)	4.6(4.7)	13.2(10.7)	4.5(2.6)	9.2(5.6)	1.4(1.4)	20.4(15.8)
CQC(n=56)	73.5(30.5)	17.2(8.2)	4.8(1.6)	6.5(6.2)	19.7(9.6)	6.1(2.7)	7.4(3.5)	0.6(0.4)	11.2(6.1)
Background sites									
XLZ(n=42)	42.6(20.1)	12.4(5.1)	1.5(0.7)	3.7(5.0)	8.4(7.0)	3.4(2.2)	5.0(2.7)	0.3(0.3)	7.9(5.6)
LAZ(n=60)	66.3(36.6)	21.7(6.5)	2.9(1.4)	8.7(8.5)	11.2(6.3)	7.3(4.5)	2.0(2.0)	0.6(0.8)	11.9(8.2)
DHM(n=36)	40.1(20.4)	11.6(5.0)	2.0(1.0)	4.5(3.9)	10.1(5.3)	4.0(1.7)	3.8(0.9)	0.5(0.6)	3.6(1.5)
NMT(n=35)	9.5(10.7)	3.4(2.7)	0.2(0.5)	0.1(0.1)	0.4(0.4)	0.4(0.2)	3.9(2.0)	0.1(0.0)	1.1(2.6)
CBM(n=52)	23.3(6.8)	8.9(3.6)	0.9(0.6)	1.1(1.4)	3.3(2.3)	1.8(0.9)	3.7(1.9)	0.2(0.2)	3.5(3.4)
GGM(n=36)	32.2(29.7)	13.1(13.5)	1.1(0.8)	0.4(0.5)	4.7(4.1)	1.7(1.3)	3.2(2.9)	0.4(1.4)	7.7(8.0)

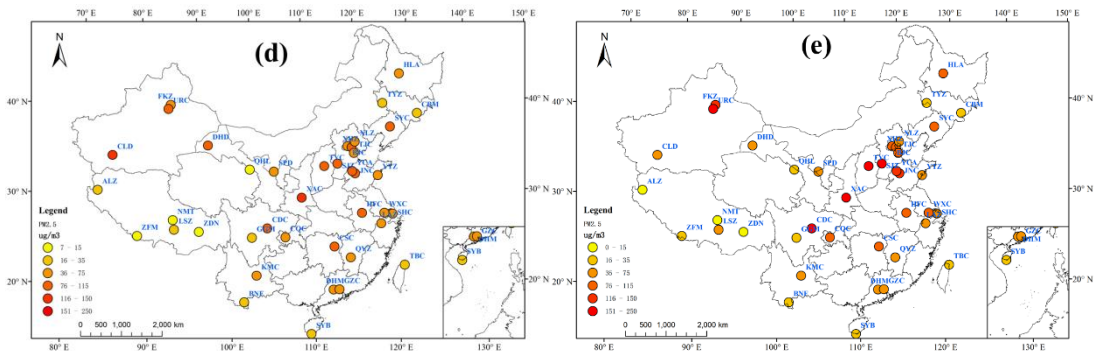
1110 \*MD: mineral dust; \*\*Unaccounted: the difference between the PM<sub>2.5</sub> gravimetric mass and the sum of the PM  
 1111 constituents (OM, EC, SO<sub>4</sub><sup>2-</sup>, NO<sub>3</sub><sup>-</sup>, NH<sub>4</sub><sup>+</sup>, Mineral dust and Cl<sup>-</sup>).  
 1112



1113



1114



1115

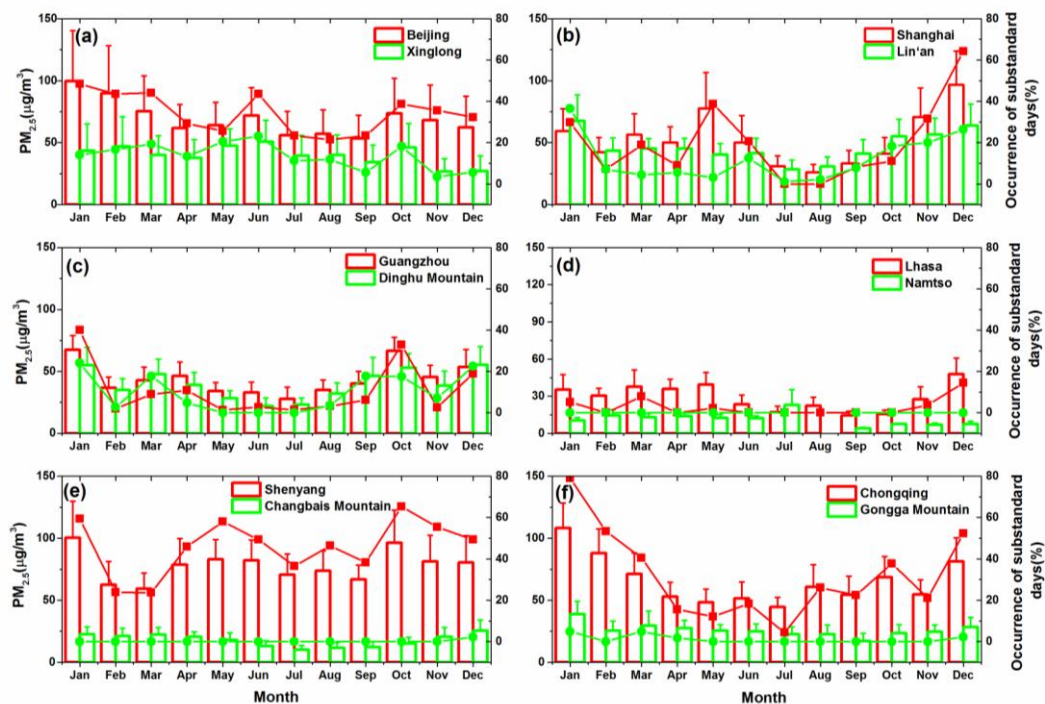
1116 Fig.1. Locations and the averaged PM<sub>2.5</sub> concentrations of the forty monitor stations during (a) the  
 1117 year of 2012-2014, (b) spring, (c) summer, (d) autumn and (e) winter. The site code related to the  
 1118 observation stations could be found in Table 1.

1119

1120

1121

1122



1123

1124

Fig.2. Monthly average PM<sub>2.5</sub> concentration (histogram, left coordinate) and the occurrence of

1125

substandard days in each month (dotted line, right coordinate) at urban and background sites in

1126

(a)North China plain, (b)Yangtze River delta, (c) Pearl River delta, (d)Tibetan Autonomous Region ,

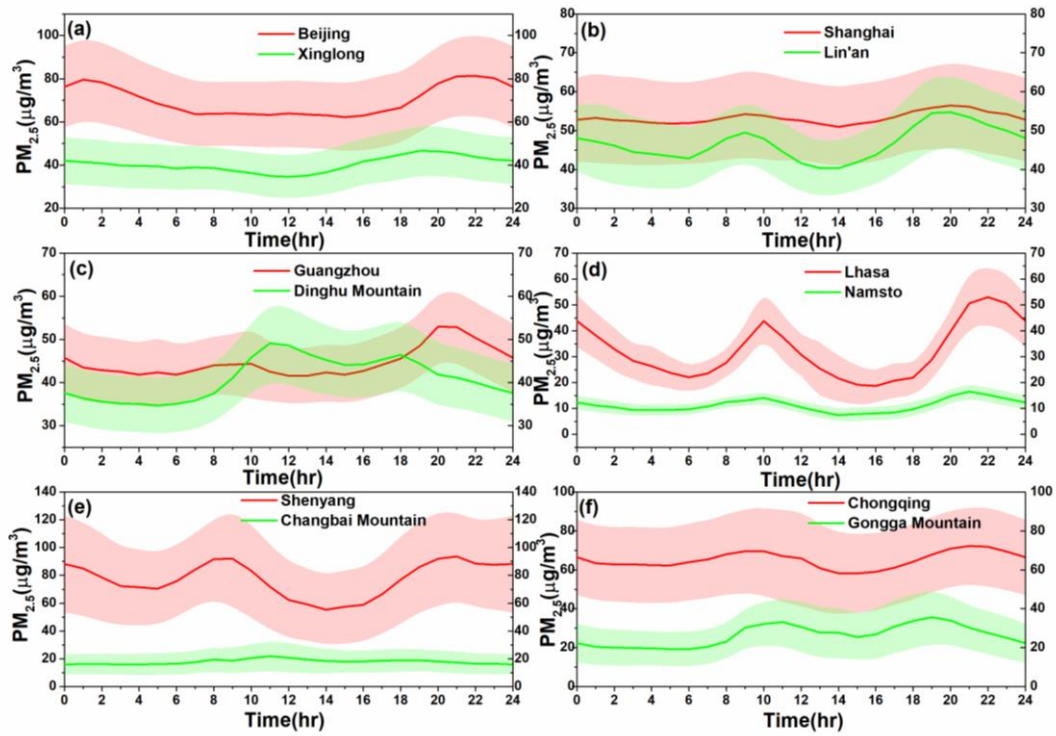
1127

(e) Northeast China Region and (f) Southwestern China Region. The error bars stands for the

1128

standard deviation.

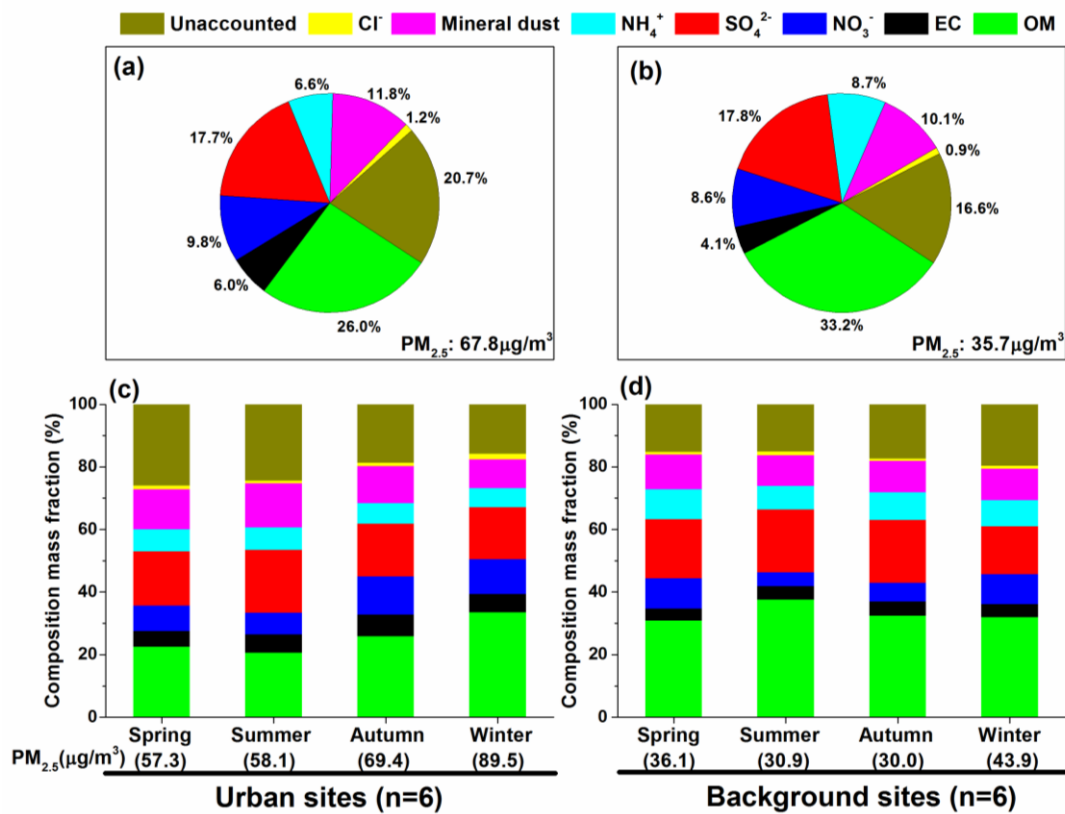
1129



1130

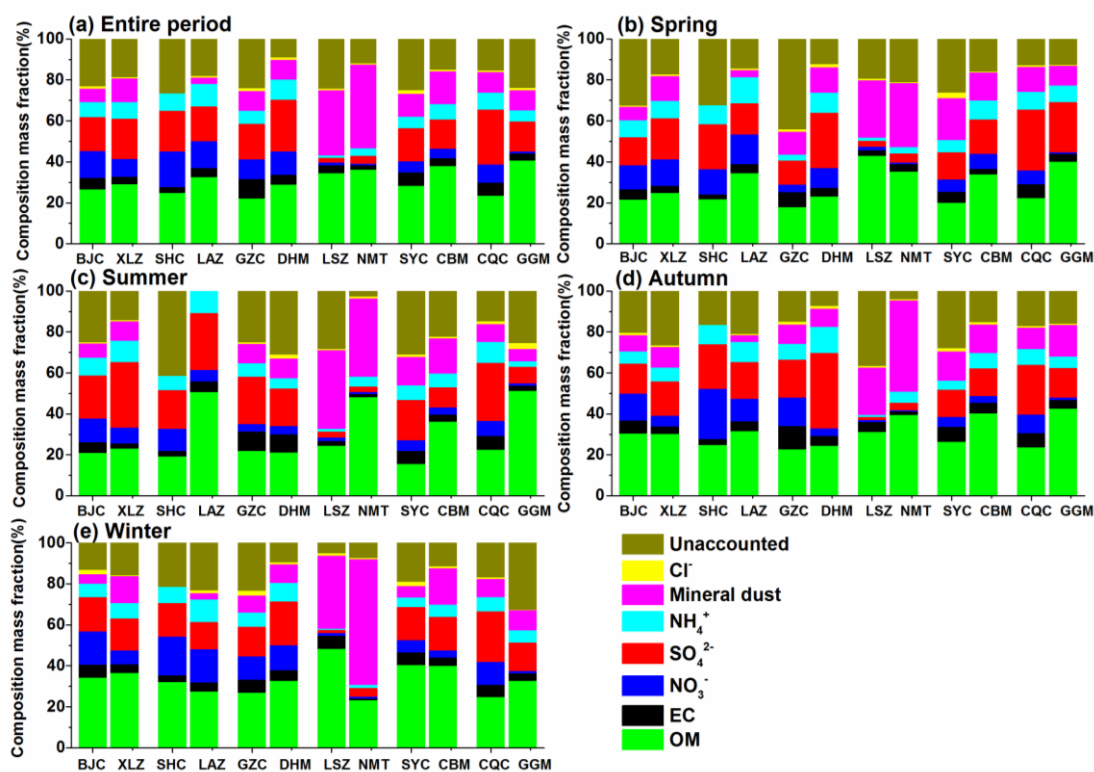
1131 Fig.3 Diurnal cycles of  $PM_{2.5}$  at six paired urban and background sites in (a)North China plain,  
 1132 (b)Yangtze River delta, (c) Pearl River delta, (d)Tibetan Autonomous Region, (e) Northeast China  
 1133 Region and (f) Southwestern China Region. Shadow area represent the error bars and stands for one  
 1134 half of the standard deviation.

1135



1136  
 1137  
 1138  
 1139  
 1140  
 1141

Fig. 4 Average chemical composition and its seasonal variations of PM<sub>2.5</sub> in (a, c) urban sites and (b, d) background sites. The unaccounted matter refer to the difference between the PM<sub>2.5</sub> gravimetric mass and the sum of the PM constituents (OM, EC, SO<sub>4</sub><sup>2-</sup>, NO<sub>3</sub><sup>-</sup>, NH<sub>4</sub><sup>+</sup>, Mineral dust and Cl<sup>-</sup>).



1143

1144

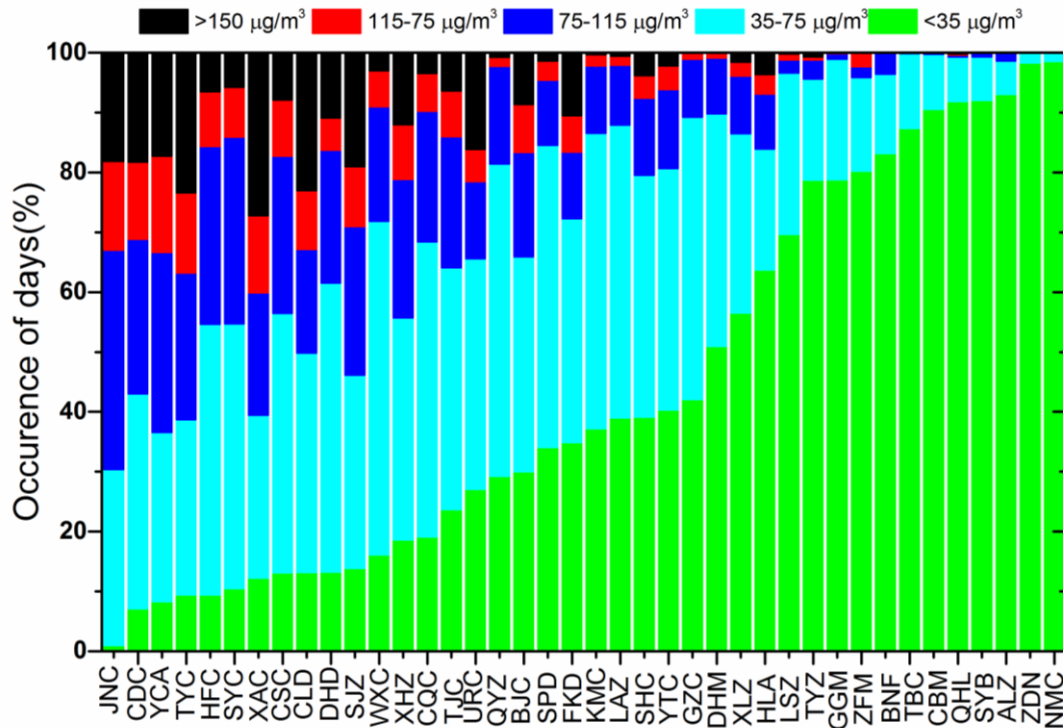
1145

1146

1147

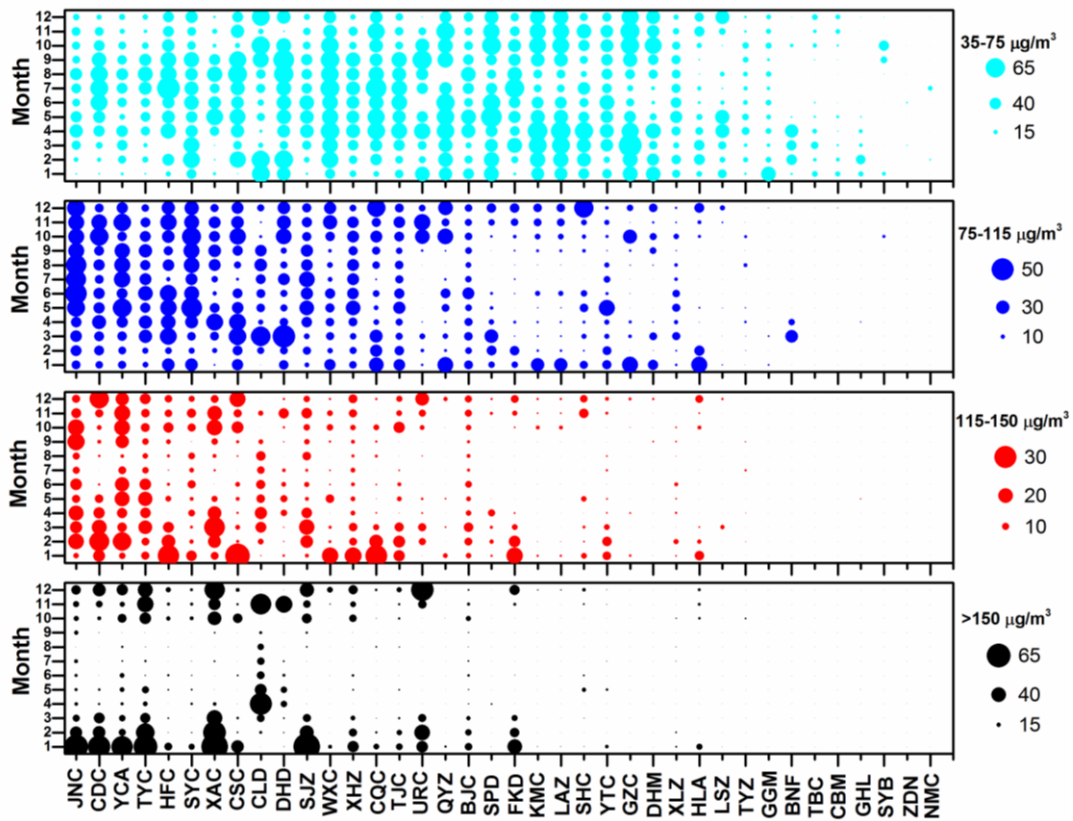
1148

Fig.5 Average chemical composition of PM<sub>2.5</sub> in individual site during (a) the entire period and (b-e) the different seasons. The unaccounted matter refer to the difference between the PM<sub>2.5</sub> gravimetric mass and the sum of the PM constituents (OM, EC, SO<sub>4</sub><sup>2-</sup>, NO<sub>3</sub><sup>-</sup>, NH<sub>4</sub><sup>+</sup>, Mineral dust and Cl<sup>-</sup>). The site code related to the observation stations could be found in Table 1.



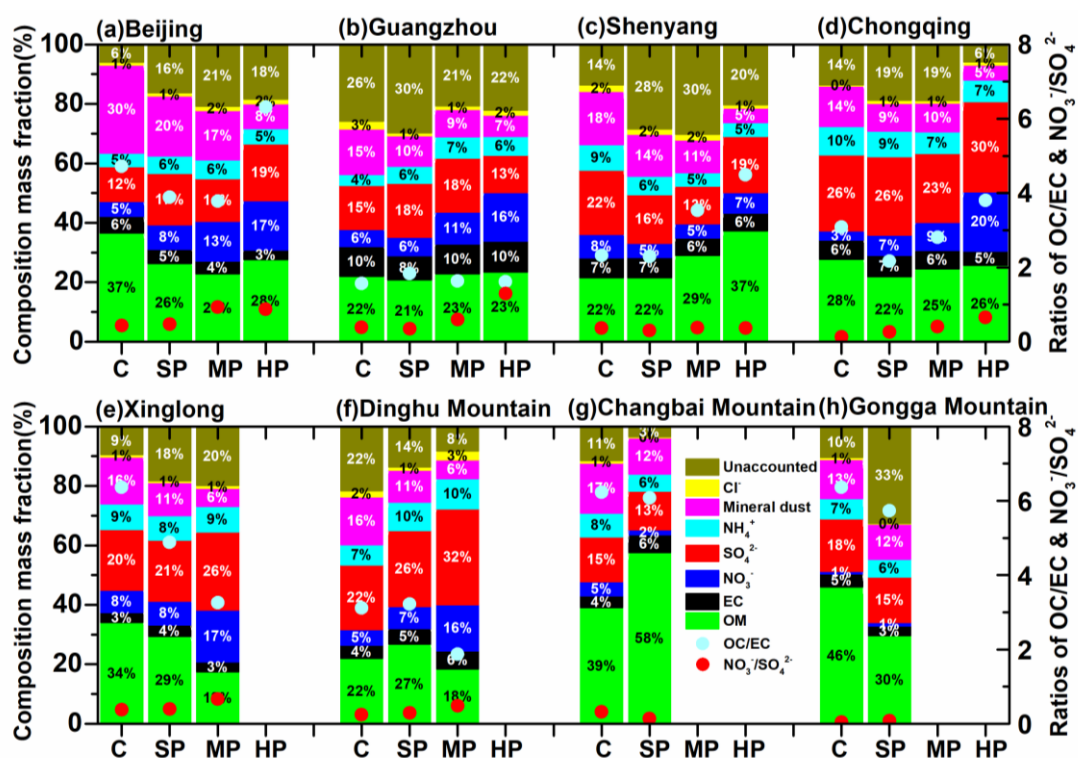
1149

1150 Fig.6 Days separated by the threshold values of the “Ambient Air Quality Standard” (AAQS)  
 1151 (GB3095-2012) of China guideline. The threshold values of 35, 75, 115 and 150µg/m<sup>3</sup> used for the  
 1152 daily concentration ranges are represented as clean (<35µg/m<sup>3</sup>), slightly polluted (35-75µg/m<sup>3</sup>),  
 1153 moderated polluted (75-115µg/m<sup>3</sup>), polluted (115-150µg/m<sup>3</sup>) and heavily polluted (>150µg/m<sup>3</sup>),  
 1154 which suggested by the guideline of the AAQS. The site code related to the observation stations  
 1155 could be found in Table 1.



1156  
 1157  
 1158  
 1159  
 1160  
 1161  
 1162

Fig.7 Monthly distribution of the occurrence of the polluted days exceeding the “Ambient Air Quality Standard” (AAQS) (GB3095-2012) of China. The symbol size represents the occurrences of polluted days for the corresponding month. The symbol color represents the different mass range. The sites of Nagri and Mount Everest are excluded because of the small sample size. The site code related to the observation stations could be found in Table 1.



1164

1165

1166

1167

1168

1169

1170

Fig. 8 Average chemical composition of PM<sub>2.5</sub> and the mass ratio of [NO<sub>3</sub><sup>-</sup>]/[SO<sub>4</sub><sup>2-</sup>] and OC/EC with respect to pollution level. The C, SP, MP and HP is related to clean (daily PM<sub>2.5</sub> < 35 μg/m<sup>3</sup>), slightly polluted (35 μg/m<sup>3</sup> < daily PM<sub>2.5</sub> < 75 μg/m<sup>3</sup>), moderated polluted (75 μg/m<sup>3</sup> < daily PM<sub>2.5</sub> < 150 μg/m<sup>3</sup>) and heavily polluted (daily PM<sub>2.5</sub> > 150 μg/m<sup>3</sup>). The unaccounted matter refer to the difference between the PM<sub>2.5</sub> gravimetric mass and the sum of the PM constituents (OM, EC, SO<sub>4</sub><sup>2-</sup>, NO<sub>3</sub><sup>-</sup>, NH<sub>4</sub><sup>+</sup>, Mineral dust and Cl<sup>-</sup>).